Session IV.

Poster Discussion

Moderators: B. Wieland, F. Helus

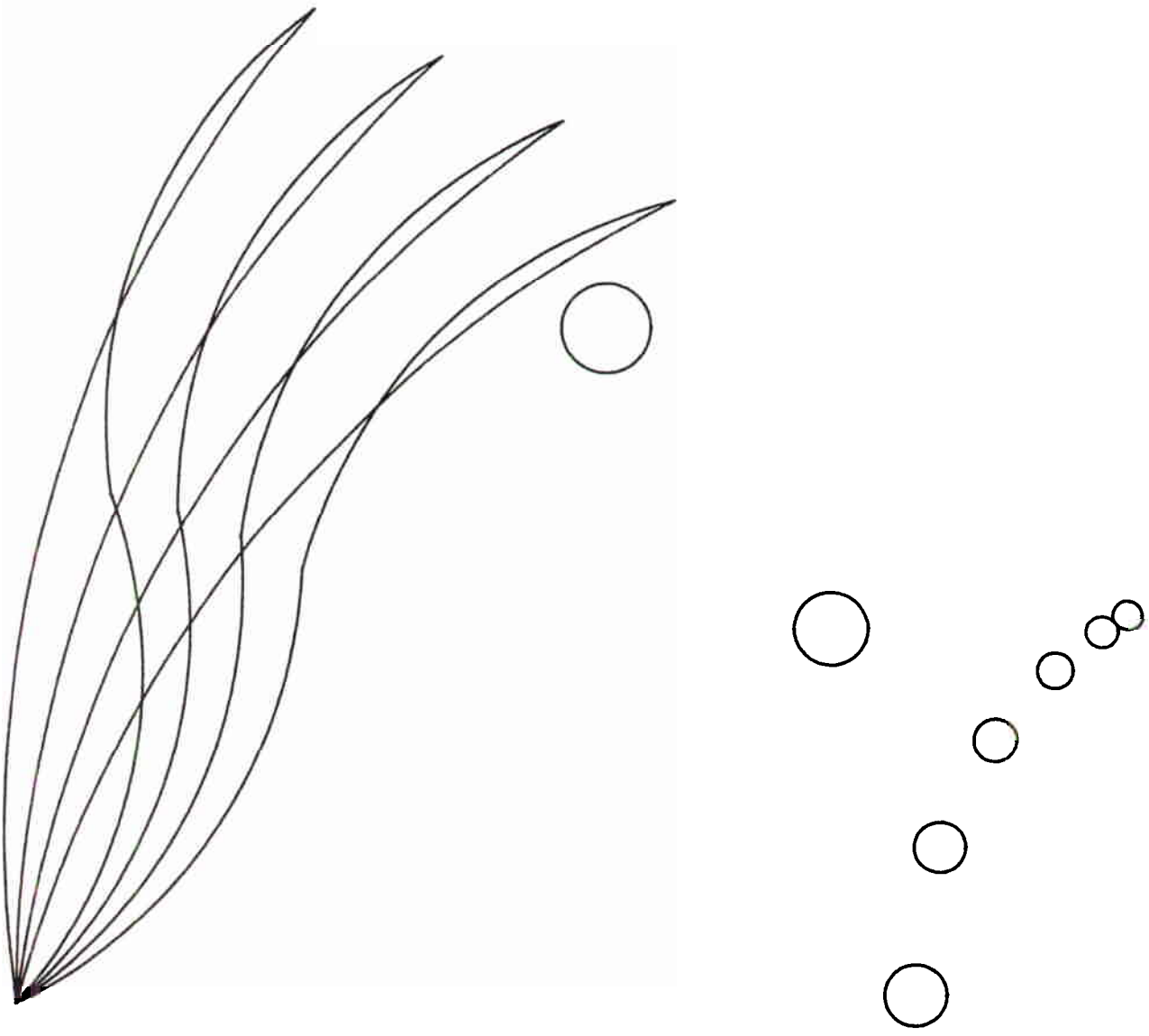

Fleas do not have wings. They travel by jumping.

Session IV Poster Discussions

Frank Helus and Bruce Wieland, Co-chairs

Session Summary

Speaker 1 - S.N. Dmitriev, Joint Institute for Nuclear Research, Flerov Laboratory of Nuclear Reactions, Moscow Russia

The first topic described the use of an electron microtron beam incident on a tantalum target chamber containing enriched ^{124}Xe. (200 atmospheres in 10 cm^3). Gammas from the tantalum produce ^{123}I in the gas from the gamma,n reactions. 200 mCi were produced after 10 hours of irradiation and 4 hours of cooling. 500 mCi are expected in the future.

The second topic was high purity ^{237}Pu (45 day electron capture decay) used for medical studies in humans (see proceedings for details).

The third topic was production of long-lived ^{26}Al for metabolic studies in humans using singly ionized alpha particles on a Mg target.

Speaker 2 - F. Helus, DKFZ Heidelberg

The presentation focussed on the effect of irradiation condition and choice of target construction materials for obtaining ^{18}F from the $^{20}Ne(d,\alpha)^{18}F$ reaction (see proceeding for details).

Roy Tillbury commented on the role played by thermal convection in the observed result that almost all the 18F activity was trapped on the upper surface of the target. He also noted that the irradiations conditions were kept constant, but the amount of activity trapped on foils in the target varied.

An unidentified participant asked about the chemical form of the recovered 18F. Work to determine this was in progress.

Speaker 3 - J.R. Dahl, North Shore University Hospital

A target system for routine production of ^{18}F via deuteron bombardment of neon for the production of electrophillic ^{18}F was presented (see proceeding for details).

The speaker made valuable observations about using the criteria of total radiation dose per molecule in order to identify the effects of parameter variations of pressure beam current, thin vs thick targets etc., and make sense out of sometimes confusing data.

There were no questions.

Speaker 4 - R.J. Nickles, University of Wisconsin, Madison

The topic presented was an evaluation of positron-emitting diffusible flow tracers for use in myocardial studies of open-chest canine preparations. A rapid flow measurement is required just before clearance measurements to study the pharmacokinetics of various new drugs. Many studies require six hours of preparation and six hours of testing. In these applications, both dissolved ^{18}F-fluoromethane and ^{14}O water were workable, with short biological half-life and short physical half-life respectively providing the basis for rapid measurements. The speaker indicated a preference for the simpler kinetics of dissolved fluoromethane. (see proceeding for details). Questions were not recorded due to technical difficulties.

Speaker 5 - E. Galiano, M.D. Anderson Medical Center

A work-in-progress project on the development of a system for the production of ^{77}Br was presented. Irradiation and chemical processing are done at the University of Texas Health Sciences Center using a 40 MeV proton beam from the cyclotron. A nearly saturated solution of sodium bromide is used for the $^{79}Br(p,3n)^{77}Kr$ which is then trapped and allowed to decay to ^{77}Br (see proceeding for details). Future goals were to increase production from the microcurie level to tens of millicuries, to achieve labelling of bromodeoxyuridine for tumor imaging, and to develop imaging techniques to reduce degradation due to the 520 keV photons which accompany the desirable 230 keV emission.

P. Salvadori (Pisa) who had experience using ^{77}Br from Julich, commented that imaging degradation was a problem, the accompanying positron radiation is a problem and that the ^{77}Br half-life is too long for therapy applications, and that deoxyuridine labelled with ^{125}I is an alternative imaging agent (although the bond strength for the bromo compound is stronger).

R. Weinreich (PSI) asked if the pellet targets were considered instead of solutions, and if the 76Br would be a possibility for imaging. The speaker replied that the chemical processing dictated the use of a solution target, and that the energy requirement for the (p,4n) producing ^{76}Br was too high for their cyclotron.

J.R. Dahl suggested the use of a higher concentration of solution (0.9 g/cc instead of 0.5-0.7 g/cc) and that the use of a titanium target chamber with tantalum windows might eliminate the corrosion problems, and that a teflon slider valve might prevent failures.

R.J. Nickles suggested that the careful stacking of two medium or high energy collimators might help diminish the image degradation phenomena mentioned above.

Speaker 6 - R. Ferrieri, Brookhaven National Laboratory

This presentation was an invited tutorial requested by B. Wieland to take advantage of the speaker's expertise on the mechanisms of organic additives to aqueous solutions for the purpose of producing in-target ammonia labeled with ^{13}N. The mechanisms of radiolytic oxidation and radiolytic reduction in situ are clearly not completely understood as evidenced by the variety of results observed by different experimenters using a wide variety of conditions.

The role of dilute ethanol in preventing radiolytic oxidation of ammonium ion back to oxides was addressed, since this was the subject of extensive discussion in the preceding session III (specific Targetry Problems). The role of ethanol acting exclusively as a hydroxyl radical scavenger has been shown to require up to 100 mM concentrations, and ammonium ion has been observed as the predominant product using 1-5 millimolar concentrations. It was therefore proposed that there may be another unidentified oxidant present, and the possible effect of ethanol (or other organic additives) is to remove this species.

The speaker presented a comprehensive list of radicals produced in irradiated water (including oxygenated water) on a very short time scale. Combining this with data on the irradiation of pure ethanol, possible mechanisms in dilute ethanol were presented. The presentation is beyond the scope of this summary, and it is hoped that the speaker will endeavor to write up his presentation with figures and tables for the workshop proceedings. He pointed out the need to asses the effects of pressure, target volume, dose, and dose rate and the presence of hydrogen and/or oxygen. These comments were accompanied with suggestions for future measurements, the goal being the delineation of conditions required for operation of reliable systems for the production of ^{13}N ammonia.

An unidentified participant made comments on his observation that there was no effects

when an ethanol system was sparged with oxygen.

M. Berridge (Case Western Reserve University) pointed out that the effect of pressure alone greatly enhances the effectiveness of ethanol in achieving a predominantly ammonium ion product. Although he observed independent dose and dose rate effects, these were both lowered by increasing pressure.

G. Bida (Biomedical Research Foundation) brought up the effect of aqueous carbon-rich environments using diamond dust or amorphous carbon in which ammonium ion is the predominant product, and inquired if this observation shed any light on the mechanism with ethanol. The speaker responded that there may be a similar common mechanism involved in both this and the ethanol system where oxidants in the system are consumed.

Targetry for the Ruthenium-97 and Tungsten-178 (Tantalum-178) Production on the Phasotron of JINR

N.G.Zaitseva, V.I.Stegailov, V.A.Khalkin, N.G.Shakun, P.T.Shishljannikov

Joint Institute for Nuclear Research, Dubna, Russia

This paper describes recent developments of the solid target system for the production of ^{97}Ru and ^{178}W in the ^{99}Tc(p,3n)^{97}Ru and ^{181}Ta(p,4n)^{178}W reactions. Radioisotope production proceeds on the internal 50–70 MeV proton beam of JINR phasotron. The target construction, condition of the irradiation and radionuclide practical yields were searched.

The decay characteristics of ^{97}Ru [$T_{1/2}$=2.9d, 100% EC, E_γ 215 keV (85.8% abundant) and 324 keV (10.2% abundant), no beta emission] and ^{178}Ta [$T_{1/2}$=9.3 m, the daughter from its parent ^{178}W($T_{1/2}$=21.7d), 98.9% EC, 1.1% β^+ emission, X-rais of ^{178}Hf with energies ranging from 54 to 65 keV] appear to be suitable for nuclear medical applications (for diagnostic imaging and therapeutic purposes).

The reactor and accelerator methods suggested so far to produce ^{97}Ru include: ^{96}Ru(n,γ)^{97}Ru, ^{103}Rh(p,2p5n)^{97}Ru, Mo(^{4}He or ^{3}He,xn)^{97}Ru. Ruthenium-97 can be produced using ^{99}Tc(p,3n)^{97}Ru reaction also. The excitation function for this reaction was determined by us for the first time (Fig.1)[1]. The maximum cross section for ^{97}Ru formation was found to be 440 mb (±15%) at 32 MeV; the yield of thick target larger than 10.5 mCi/μAh may be achieved for E_p=100 MeV.

The production of ^{97}Ru can be performed with medium sized cyclotrons, for E_p=50 MeV and ~3 g/cm^2 Tc target about 7 mCi/μAh of ^{97}Ru may be produced. The ^{97}Ru yield increases only for 15% at E_p=60 MeV but in this case summary activity of target increases several times as much.

Tantalum-178 can be produced from a generator following the reaction ^{181}Ta(p,4n)^{178}W$\rightarrow$ $\underset{21.7days}{\overset{EC}{\longrightarrow}}$ ^{178}Ta $\underset{9.3min}{\overset{EC,\beta^+}{\longrightarrow}}$ ^{178}Hf (stable). The excitation function for this reaction was measured by us over the proton energy range of 29–72 MeV (Fig.2)[2]. The maximum cross section is 495 mb (±15%) and occurs at 40 MeV. The experimental results show that ^{178}W yield is approximately same both the maximum region (30 MeV$\leq E_p \leq$50 MeV) and tail one of the excitation function (50 MeV$\leq E_p \leq$70 MeV). So we have decided to use rather thick Ta targets (6.5–7 g/cm^2) for irradiation by protons with 70 MeV energy on internal phasotron beam.

JINR phasotron is not adapted for routine isotope production. But it has remotely controllen probe and so it is possible to irradiate radiochemical targets inside an accelerator vacuum chamber by protons of given energy in the range from 20 to 600 MeV at the 6–8 μA intensity.

There is not high current accelerators with proton energy $\geq$40 MeV in Russia. So the application of phasotron to obtain 100–150 mCi ^{97}Ru and ^{178}W regularly is worth while to carry out medical, biological and radiopharmaceutical experiments.

An activation process of targets on the phasotron internal beam has some peculiarities. Nuclear reaction products are concentrated in primary millimeters of target in radial direction (Fig.3). This zone size dependes on target high and thickness. Vertical distribution of inside beam intensity measured after irradiation of 4 g/cm^2 copper target by protons with energy 50 and 70 MeV is shown in Fig.4.

Experimental data of excitation function of (p,3n) and (p,4n) nuclear reactions on ^{99}Tc and ^{181}Ta and of distribution of proton beam on targets were applied to design of metal Tc and Ta targets (Fig.5). They consist of three plates (1×10×2.6 mm for Tc and 1×10×4 mm for Ta) pressed on water coold head of the stock. A distance between plates is 1.5 mm, Tc mass is ~1 g, Ta mass is ~2 g. Such targets construction have to intercept about 80% proton beam. It also is important that such disposition of Tc plates excludes their heating by proton beem to melt temperature (~2500 K) and so excludes metal loss because of its vacuum evaporation. For such target construction irradiated metals are separated easily from holder by remote tools.

Quantities of ^{97}Ru and ^{178}W realy obtained during one hour irradiation were determinated at exposition from 10 to 30 min at ~8 μA current of protons.

As it was expected the productions were rather high: 40–50 mCi/h for ^{97}Ru and 5–6 mCi/h for ^{178}Ta. These values were measured by gamma-spectrometric method.

It was neccessary to have effective radiochemical methods of separation of ^{97}Ru and ^{178}W from target materials. For ^{178}W they are worked out and descripted in detailes [3]. To separate a carrier free ^{97}Ru and macro amounts of Tc we used known property of RuO_4 to be distillate from acids. Our primary researches have showed that it is possible to separate Ru from solutions of 0.1–0.05 mol/l $HTcO_4$ in H_2SO_4 and $HClO_4$ containing oxidation agents and if the Tc solutions are free of nitrate and chloride ions. It is possible to separate about 90% of ^{97}Ru during 3 hours distilation in air streem from solutions heated to $\leq$100°C. Under such conditions Tc does not distilled and it does not been discovered in ^{97}Ru solution (HCl–H_2O_2). A report devoted to obtained of ^{97}Ru preparations is under development.

References

[1] N.G.Zaitseva, E.Rurarz, M.Vobecky et al., "Excitation function and yield for ^{97}Ru production in ^{99}Tc(p,3n)^{97}Ru reaction in 20–100 MeV proton energy range", Radiochim. Acta 56 (1992) 59.

[2] N.G.Zaitseva, E.Rurarz, V.A.Khalkin et al., "Excitation function for ^{178}W production in the ^{181}Ta(p,4n)^{178}W reaction over proton energy range 28.8–71.8 MeV", This Proceed.

[3] R.D.Neirinckx, M.A.Davis and B.L.Holman, "The ^{178}W/^{178}Ta generator: anion exchange behaviour of ^{178}W and ^{178}Ta", Int. J.Appl. Rad. and Isotopes 32 (1981) 85.

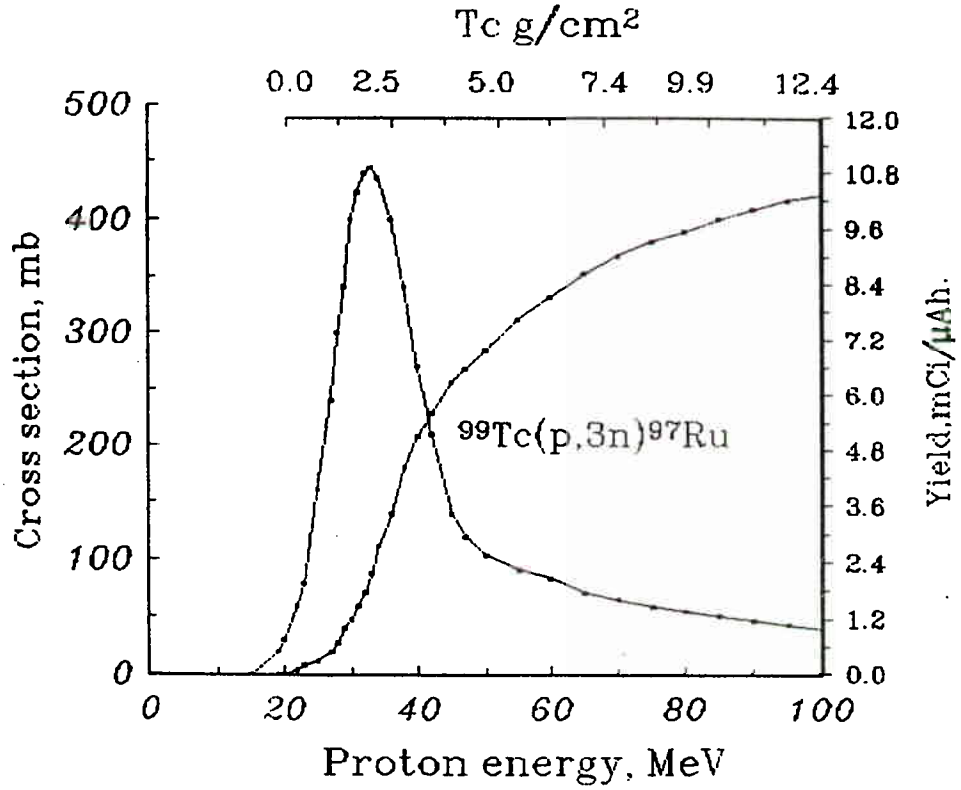

Fig. 1. Cross section and cumulative yield of proton induced $^{99}Tc(p,3n)^{97}Ru$ reaction.

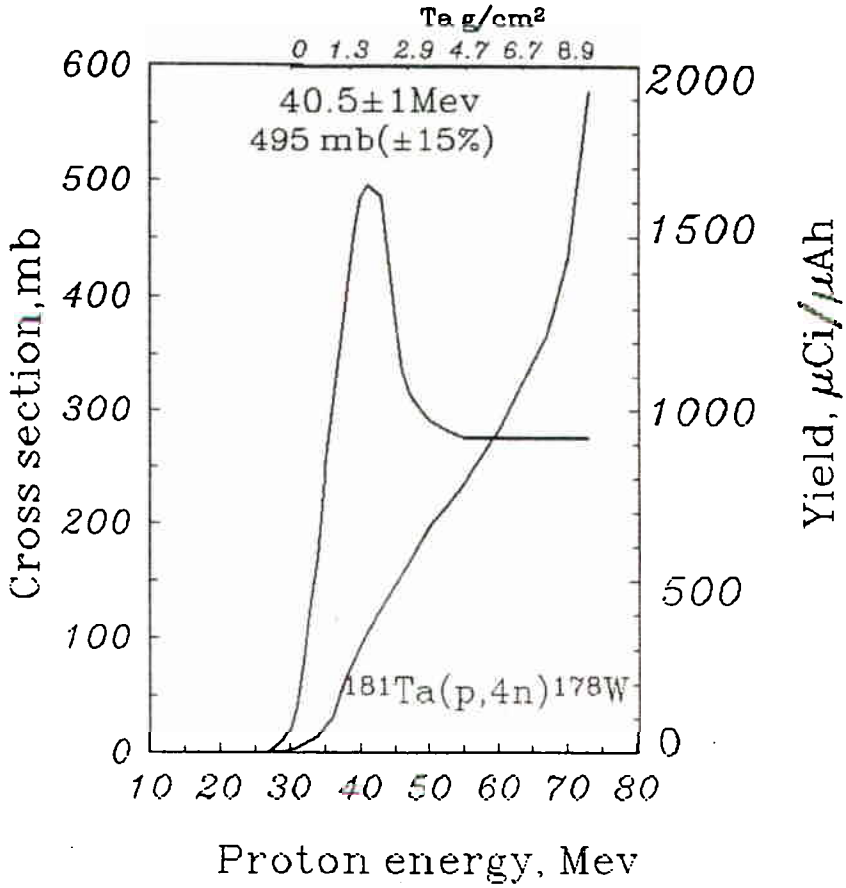

Fig. 2. Cross ssection and cumulative yield of proton induced $^{181}Ta(p,4n)^{178}W$ reaction.

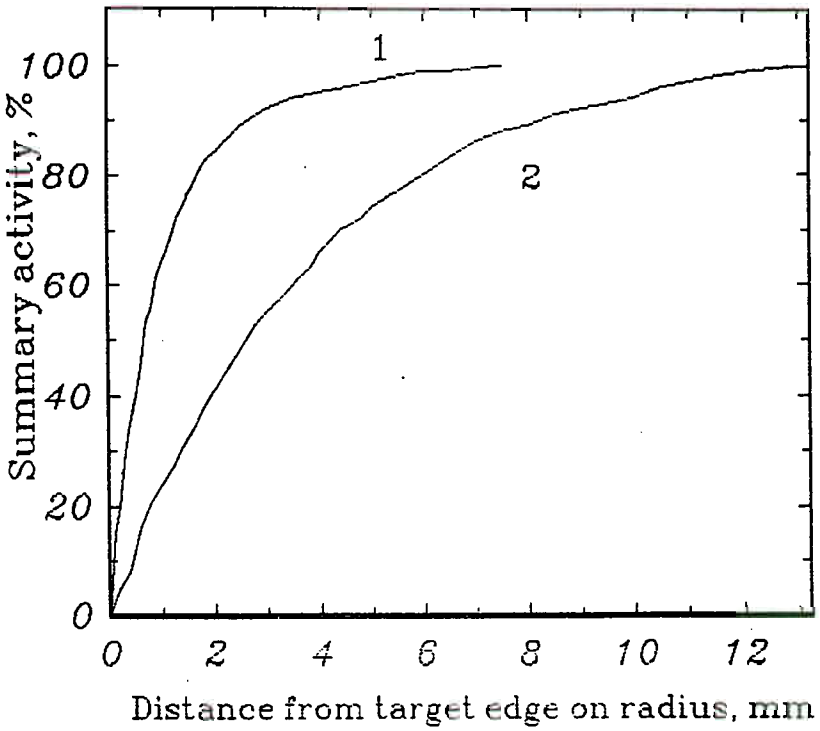

Fig. 3. Activity distribution as a function of radial depth of thick target under internal proton beam irradiation with 50 and 70 MeV energy at LNP Phasotron: 1— Al target, 5 g/cm^2, h=15 mm; 2— Cu wire, d=1.75 mm.

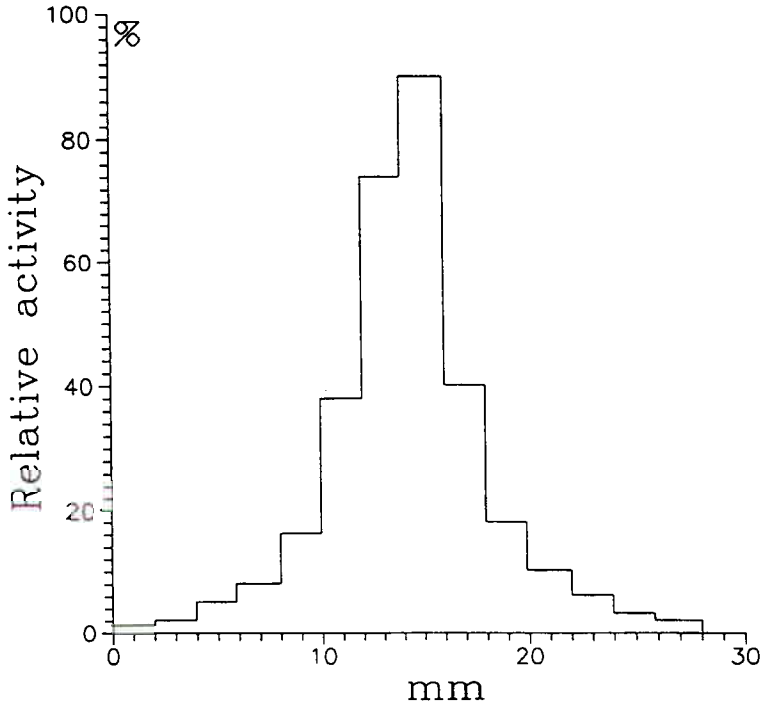

Fig. 4. Vertical distribution of internal proton beam intensity: E_p=60±10 MeV; Cu target, 4 g/cm^2.

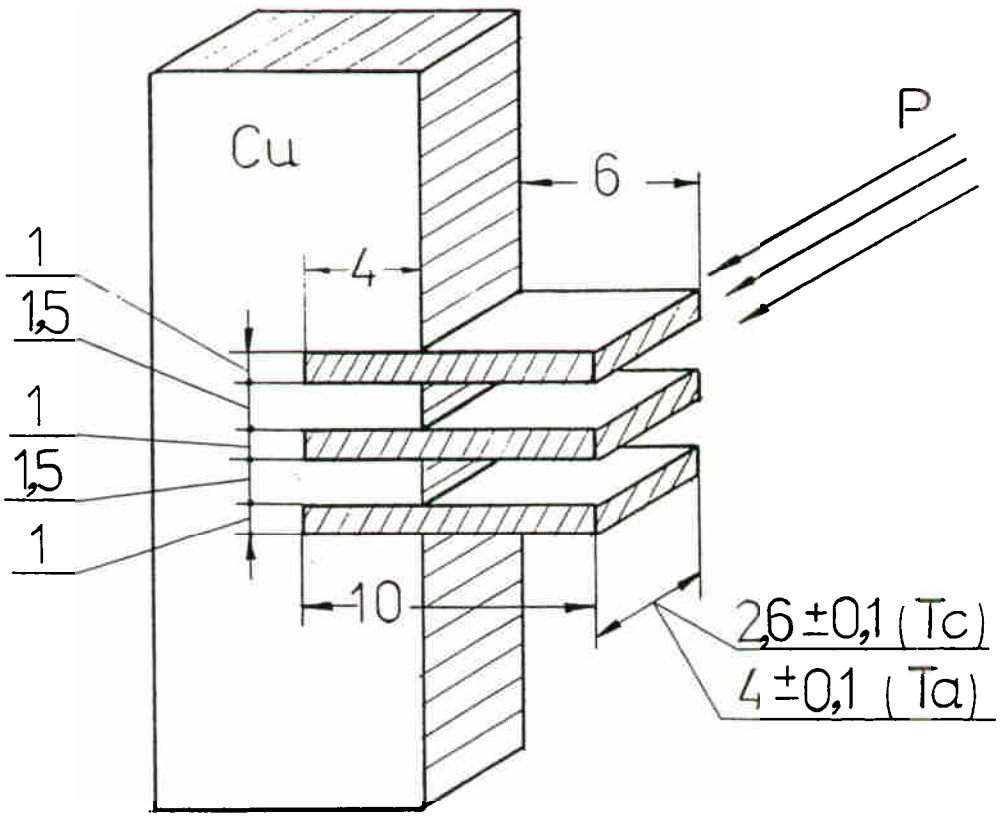

Fig. 5. Target assembly mounted for irradiation.

Excitation Function for ^{178}W Production in the ^{181}Ta(p,4n)^{178}W Reaction over Proton Energy Range 28.8–71.8 MeV

By N.G.Zaitseva[1], E.Rurarz[2], V.A.Khalkin[1], V.I.Stegailov[1] and L.M.Popinenkova[3]

[1] *The Joint Institute for Nuclear Research, Dubna, Russia*
[2] *The Soltan Institute for Nuclear Studies, Swierk, Poland*
[3] *The Institute for High Energy Physics, Serpukhov, Russia*

1. Introduction

Among the more attractive radionuclides for lung and liver imaging in children and adults, particularly in cardiovascular examinations, is ^{178}Ta [1-3]. This radionuclide is readily available from the radionuclide generator $^{178}W \xrightarrow[T_{1/2}=21.7d]{EC} {}^{178}Ta \xrightarrow[T_{1/2}=9.3min]{EC,\beta^+} {}^{178}Hf$ (stable). The long lived ^{178}W ($T_{1/2}$=21.7d) decay entirely by EC to 9.3 m ^{178}Ta daughter without feeding the high spin isomer ($T_{1/2}$=2.2 h) in ^{178}Ta [4,5]. The short lived ^{178}Ta then decays to stable ^{178}Hf, 98.92% by EC and 1.1% by β^+ emission.

The decay characteristics of ^{178}Ta [6] appear to be suitable for nuclear medical applications in conjunction with a low energy detection system, such as the MWPC (a high-pressure Multi-Wire Proportional Camera) which is efficicent for detection of 55-94 keV X and γ rays [7,8].

The short physical half life of ^{178}Ta permits multiple sequential studies with reduced patient radiation dose compared with the current radionuclide of choice, i.e. ^{99m}Tc and warrants improved spatial resolution.

The ^{178}W production can be achieved in various nuclear reactions:

1) $^{177}Hf(^3He,2n)^{178}W(E_{thr} = 3.7\ MeV)$,
2) $^{178}Hf(^3He,2n)^{178}W(E_{thr} = 11.5\ MeV)$,
3) $^{176}Hf(^4He,2n)^{178}W(E_{thr} = 18.3\ MeV)$,
4) $^{181}Ta(d,5n)^{178}W(E_{thr} = 25.5\ MeV)$,
5) $^{181}Ta(p,4n)^{178}W(E_{thr} = 23.1\ MeV)$.

If protons of suitable energy are available, their use is preferred since the yields are higher in comparison with ^{3,4}He–induced reactions due to a larger range of penetration. At present, the parent nuclide ^{178}W is produced almost exclusively in the ^{181}Ta(p,4n)^{178}W reaction although the data are fragmentary and sparse [9,10,11].

In this paper we report excitation function for the ^{181}Ta(p,4n)^{178}W reaction in the proton energy range of 28.8-71.8 MeV.

Comparison with theoretical calculations of the excitation function based on the concept of a hybrid model of nuclear reactions (in the from of Overlaid Alice code) is shown.

2. Experimental

High purity natural Ta(^{180}Ta 0.0123%, ^{181}Ta 99.8877%) in metallic form was used as a target material. The excitation function of the ^{181}Ta (p,4n) reaction was measured using a stacked foil technique.

The external 73 MeV proton beam of the linear accelerator (LU–100) at the Institute for High Energy Physics in Serpukhov (Russia) was used for irradiation. The Al colimator was used to assure that all of the induced radioactivity in the foil was concentrated in a small but well defined area. The degradation of the proton energy passing through Ta stack was calculated using the range-energy tables [12]. The proton flux was determined via monitor reaction on Al foils. The stack was irradiated for 12 hours with a proton beam current of ~40 nA. After irradiations, the stacks were repeatedly measured over a period of several months using a computerized γ–spectroscopy system.

^{178}Ta in secular equilibrium with ^{178}W has prominet γ–rays with energies 1341 keV (1.02%), 1350 keV (1.18%) and 511 keV annihilation radiation due to the 1.1% positron branch. These lines decayed with 22 day parent half life and were used for cross section determinations, contrary to all previous works [9-11] where the X–ray lines were used to evaluate the cross sections. The spectroscopic data used in this work were taken from two standard works [4,5].

The number of counts in the relevant photopeak areas for the measured γ–ray spectra and absolute activities (with the known number of atoms in target foils and beam intensities) were then used to determine the cross section values. The total errors in the cross section (~15%) were obtained, as described earlier [13]. Theoretical excitation functions were calculated with the Overlaid Alice code [14] for the ^{181}Ta(p,xn)$^{182-x}$W (x=1;3–8) reactions from thresholds up to 100 MeV proton energy on the CDC–Cyber computer of the Institute of Atomic Energy in Swierk (Poland).

3. Results

The results are given in Table 1 and Fig. 1. Our measurements indicate that the maximum cross section of the excitation function is (495±74 mb) and occurs at 40 MeV.

For the sake of completeness and for comparison, the values reported earlier are also shown [9-11]. The overall agreement between theory and experiment is well within the factor of 2, which is currently the best the that can reasonably be expected of all the Alice codes [15]. It can be seen from Fig.1 that the excitation function calculated with the Overlaid Alice code reproduces the shape of the experimental data reasonably well except for the high energy tail of experimetnal data (the effects of preequilibrium processes). There exists a 4 MeV displacement of the calculated peak position of the excitation function with respect to the experimental values. This displacement was already observed earlier by other users of the Alice code [16].

Thick target yields have been obtained by integrating the excitation function over the energy region of interest. In this manner, ^{178}W yield larger than 1.3 mCi/μAh may be achieved, which permits the production of several handred milicuries of ^{178}W per day, if more than 10 μA of 70 MeV proton beams are available.

4. Conclusion

The present work describes the excitation function for the ^{181}Ta(p,4n)^{178}W reaction in the 28.8-71.8 MeV proton energy range. This information was previously not known accurately and will be valuable to the users of medical cyclotrons.

The ^{178}W may be produced in the entire energy range stuied. No other tungsten radioisotopes were detected.

Some disadvantage of this production method of ^{178}W lies in the fact that about 70 MeV (or greater) proton beam is needed. However, such a high energy of protons should not be a limitation of this method.

References

[1] B.L.Holman, R.D.Neirinckx, S.Treves and D.E.Tow, "Cardiac imaging with ^{178}Ta", Radiology 131, 525 (1979).

[2] R.D.Neirinckx, B.L.Holman, M.A.Davis and R.E.Zimmerman, "^{178}Ta labelled agents for lung and liver imaging", J.Nucl. Med. 20, 1176 (1979).

[3] R.A.Wilson, S.Y.Kopiwoda, R.J.Callahan et al., "Biodistribution of ^{178}Ta: a short lived radiopharmaceutical for blood pool imaging", Eur. J.Nucl. Med. 13, 82 (1987).

[4] C.M.Lederer and S.V.Shirley, "Table of Isotopes", 7-th Ed. J.Wiley, N.Y. (1978).

[5] U.Reus and W.Westmeier, "Atomic Data and Nuclear Data Tables", Part I and II, 29, No 1 and 2 (1983).

[6] H.Nielsen, K.Wilsky and J.Zylicz, Nucl.Phys. A 93, 401 (1967).

[7] R.E.Zimmerman "Advances in nuclear medicine imaging instrumentation", Proc. IAEA Symposium, Los Angeles (1976) IAEA Vienna, 1976, p.121-160.

[8] J.L.Lacy, A.D.Leblanc, J.W.Babich et al., "A gamma camera for medical applications using a multiwire proportional counter", J.Nucl. Med. 25, 1003 (1984).

[9] C.L.Rao and L.Yaffe "Nuclear reactions induced in Ta by protons of energy up to 84 MeV", Can. J. of Chemistry 41, 2516 (1963).

[10] F.Hermes "Messung von Anregungsfunctionen am Ta mit Einschussenergien bis 104 MeV und ihre Berechung nach dem statistischen Modell" Thesis, University of Bonn (1970).

[11] C.Birattari, E.Gadioli, A.M.Grassi Strini et al., "(p,xn) reactions induced in ^{169}Tm, ^{181}Ta and ^{209}Bi with 20 to 45 MeV protons", Nucl. Phys., A 166, 605 (1971).

[12] J.F.Janini "Atomic Data and Nuclear Data Tables, proton range-energy tables, 1 keV–10 GeV", part 2, Elements vol.27, No 4/5 (1982).

[13] N.G.Zaitseva, E.Rurarz, V.A.Khalkin et al., Appl. Radiat. Isot. 41, 177 (1990).

[14] M.Blann, Overlaid Alice code, COO-3494-29, Rochester University Report (1976).

[15] M.Blann et al., "Calculation and computer file of excitation functions" in Proc. IAEA, Consultants Meeting on Data Requirements of Medical Radioisotope Production, Report INDC(NDC)–195/GZ, p.17, Ed. K.Okamoto, IAEA, Vienna (1988).

[16] R.Michel et al.: Z.Phys. A 286, 393 (1978), Nucl. Phys. A 322, 40 (1979), ibid A 338, 167 (1980), ibid A 404, 77 (1982), Int. J.Appl. Radiat. Isot. 34, 1325 (1983) and Nucl. Phys. A 441, 617 (1985).

Table 1. Experimental and theoretical cross sections for the ^{181}Ta (p,4n) reaction as a function of proton energy.

E_p (MeV)	THIS WORK		BIRATTARI et al. [11]	RAO AND YAFFE [9]	HERMES [10]
	in our* stack	σexp ±15%	σ **exp±20%	σexp±22%	σ ***exp
25			48		
27.5			347		
28				140	
	28.8	11			
30			915	380	240	133±30
	30.1	28			
	31.7	81			
32				580	
32.5			1080		
	33.0	144			
34				700	
	34.2	221			
35			1160		
	35.7	305			
36				780	760	
	36.9	388			
37.5			856		
38				740	
	38.1	406			
	39.1	484			
40			647			964±62
	40.1	495			
	41.1	495			
42				460	430	
	42.1	485			
42.5			409		
	43.7	410			
44				350	
45			347		
	45.3	375			
	47.0	320			
47.5			251		
48					200	
	48.8	320			
50			241			238±30
	50.4	285			
	52.0	305			
	53.6	290			
54					130	

E_p (MeV)	THIS WORK		BIRATTARI et al. [11]	RAO AND YAFFE [9]	HERMES [10]
	in our* stack	σexp ±15%	σcalc	σ **exp±20%	σexp±22%	σ ***exp
55			190			
	55.1	295				
	56.6	325				
	58.1	277				
	59.6	280				
60			157			35±11
	61.0	275				
	62.5	295				
	63.9	270				
64					120	
65			131			
	65.3	275				
	66.7	290				
	68.0	255				
	69.0	280				
70			109			
	70.5	285				
	71.8	285				
74					62	
75			89			
80			71			
84					64	
85			56			
90			45			
95			38			
100			31			

* Average proton energy at the mid thickness of Ta foil.

** Estimated from figure 4a Ref [11].

*** Cross sections are given in CM system but for protons and for target mass 181 $E_p^{CM} \cong E_p^{LAB}$.

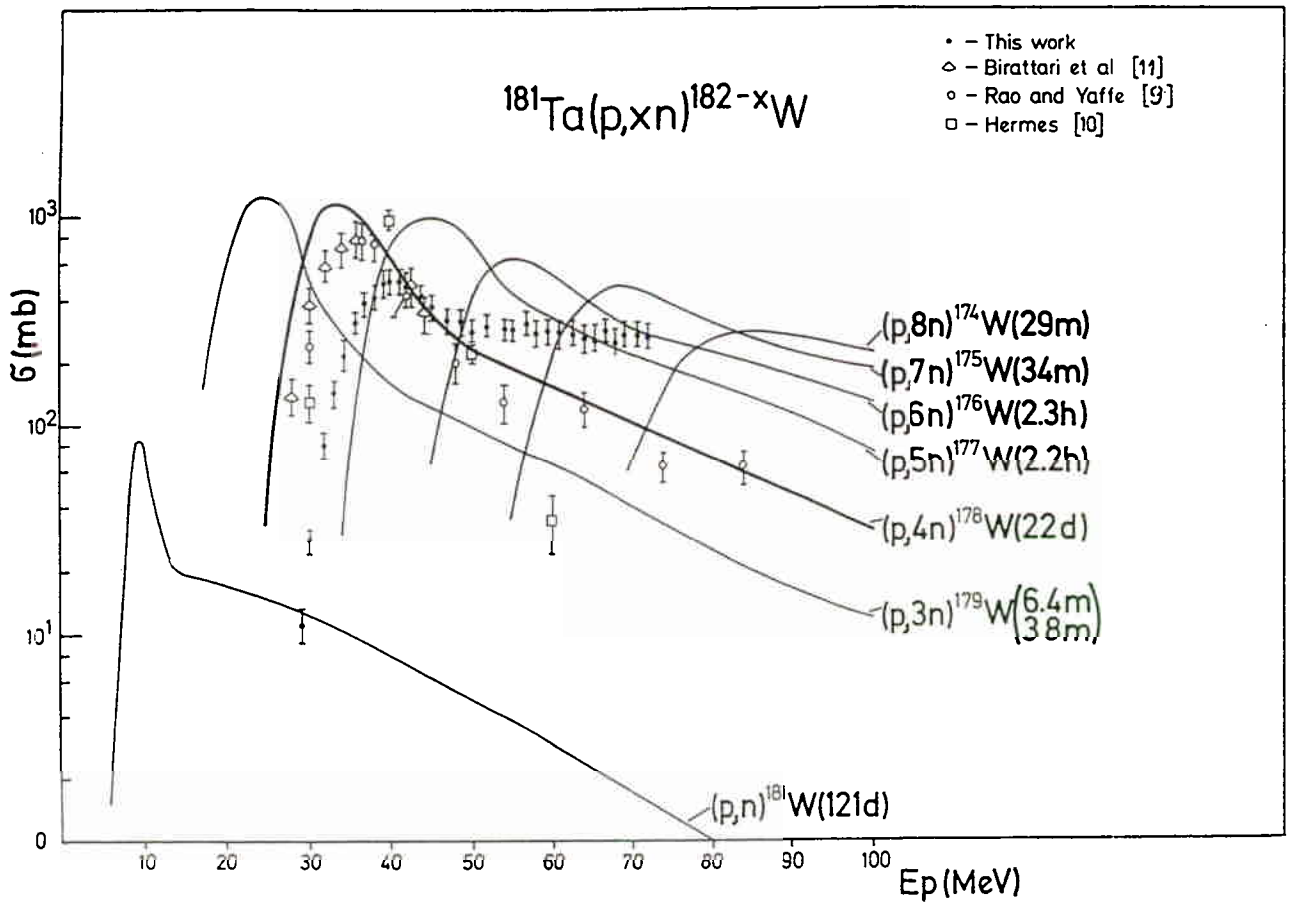

Fig. 1. Experimental and theoretical cross sections for production of ^{178}W in the ^{181}Ta (p,4n) ^{178}Ta reaction. The values of cross sections reported earlier for this reaction in Refs. [9-11] are also shown. The theoretical excitation function (continuous lines) calculated with the Overlaid Alice code for the ^{181}Ta(p,xn)$^{182-x}$W (x=1;3–8) reaction are shown. At a given energy range (25–100 MeV) calculated cross sections for the ^{181}Ta(p,4n)^{178}W reaction are shown as a thick continuous line.

A TARGET CHAMBER FOR THE ROUTINE PRODUCTION OF [^{18}F]-F_2.

J.R. Dahl, A. Belakhlef, R.A. Matacchieri, T.C. Chaly, J. Koziorowski*,. D. Margouleff,
North Shore University Hospital/Cornell University Medical College, Manhasset N.Y.,
*Scanditronix, A.B., Uppsala, Sweden,

INTRODUCTION

[^{18}F]-F_2 continues to provide a convenient route for the preparation of ^{18}F labeled compounds, particularly in the early developmental stages when the labeled compound of interest is not easily prepared by nucleophilic substitution and has yet to be shown sufficiently important to justify development of nucleophilic methods for its preparation. Although negative ion cyclotrons are currently popular as devices for producing radionuclides, a number of laboratories have positive ion cyclotrons. Some of these positive ion cyclotrons have beam transport systems, and others mount the targets directly on the cyclotron beam exit port. The result is a variety of beam profiles for bombardment of the target. Due to the smaller cross sectional area of the beam profile which may result when the target is mounted at the end of a beam transport line, a target chamber optimized for use with a cyclotron equipped with a beam transport system may not be optimal for use on a cyclotron with the targets mounted directly on the beam exit port, even though the machines may be otherwise similar. This situation poses the problem: Design a target chamber with sufficient reliability and yield to allow pursuit of a clinical research program dependent upon [^{18}F]-F_2 as a radio-labeling precursor and which works well when mounted directly on the beam exit port of a positive ion cyclotron or when mounted at the end of a beam transport line. Such a target will be suitable for use with either a circular beam entrance window for use on a beam line, or with a beam entrance window for the horizontally elongated beam obtained at the beam exit port. The fundamental parameters for the production of [^{18}F]-F_2 have been well investigated[1-5] and provide the basis for selection of the parameters used in the design of this target system. A previous design[5], specifically for use with a beam transport system, used a conical target chamber interior shape to minimize the volume of the system, thereby improving the specific activity of the [^{18}F]-F_2 by reducing the amount of added carrier. Experience with the conical target chamber configuration installed directly on the cyclotron beam exit port provided smaller yields compared to those obtained with the target mounted at the end of a beam pipe, due to beam striking the sides of the target[6]. Studies in which the volume of excited gas has been observed by photographing the light emitted by de-excitation of the plasma volume indicate the plasma shape approximates a cone[7]. There was also the speculation that some of the problems encountered by users other than the designer could be attributed to the close proximity of the edge of the plasma volume to the target chamber walls. Therefore, surrounding the active plasma with a blanket of gas may reduce the tendency of fluorine to stick to the target chamber walls by decreasing the average impact energy.

MATERIALS AND METHODS

The target system design described in this work consists of an inner nickel cylinder surrounded by a cooling water jacket, and the associated stainless steel (SS) valves, transport lines, and gas cylinders. A diagram of the target chamber assembly is shown diagrammatically in Figure 1. Electroform target bodies were prepared by A.J. Tuck Inc., of

Brookfield Connecticut by a proprietary process using aluminum mandrels on which the bodies were formed and finished. A uniform wall thickness of 1.8mm was obtained. Two lengths of target body were prepared, one which resulted in a total target inside length of 14.75 cm, shown in figure 1 by normal section view, and the other, 5 cm shorter, shown by dotted lines. When the targets were used at the end of a beam transport line, 1.9 cm circular entrance and exit windows of HAVAR, each 0.0025cm thick, were used. For experiments in which the targets mounted directly on the cyclotron beam exit port, the entrance and exit windows were 1 cm high X 3 cm by long. Experiments with the long target body have been performed with the target mounted directly on the cyclotron beam exit port and on the end of the beam line. Experiments with the short target chamber have only been performed with the target chamber mounted on the end of the beam line, consequently this comparison of the two targets is limited to experiments at the end of a beam line. Both the beam exit and target entrance foils were cooled with high-velocity recirculating helium blowing between. A Scanditronix MC17F cyclotron (E_{deut}=8.5 MeV) was used in all experiments. The larger dead volume of cooling water inside the cooling shroud with the shorter body has no significant effect since the flow through shroud with both the long and the short versions of the electroform is the same. The targets were ultrasonically cleaned using an acidic phosphate based cleaner, then, after thorough rinsing with de-ionized water, allowed to air dry in a low dust area and assembled with normal precautions to insure cleanliness.

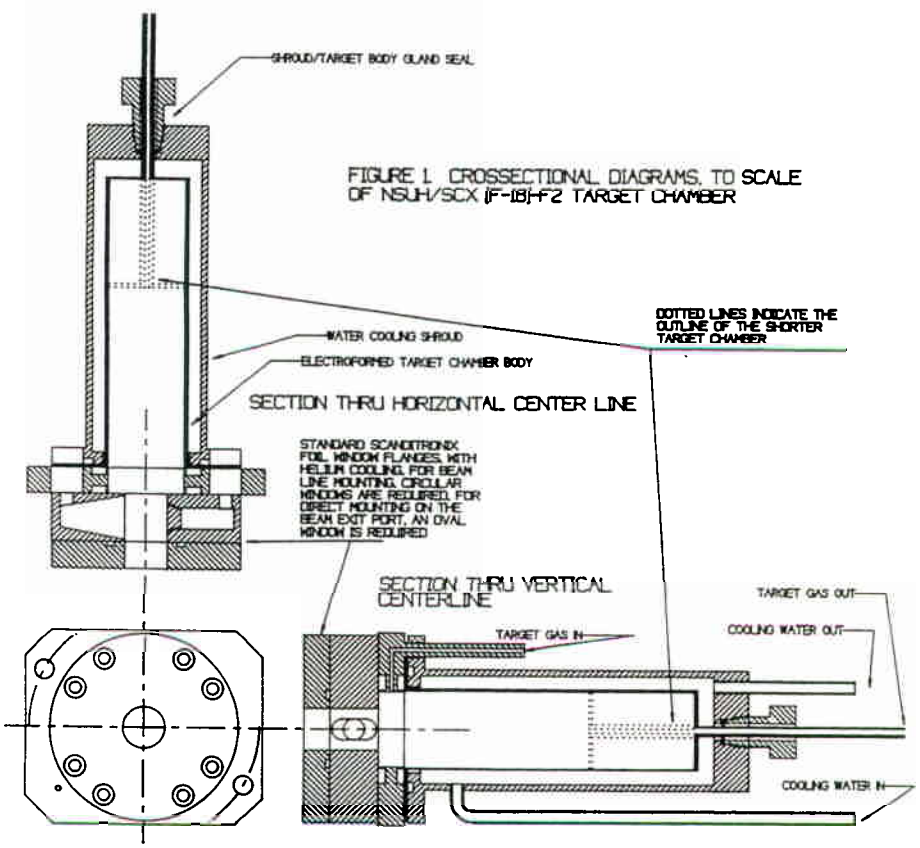

A diagram showing the general arrangement of the valves, tubing, and gas flow are shown in figure 2. The bombardment gas is prepared by combining appropriate amounts of research grade neon and 1% F_2 in research grade neon. The delivery of these gases to the target is controlled by selecting the appropriate gas by means of the gas selector valve and opening V18 until a pre-determined pressure is indicated by the pressure transducer. Flow out of the target chamber is controlled by V17. A supply of high-purity helium is connected to the system through the fluorine regulator, which is supplied with a connection to allow the system to be decontaminated before changing cylinders or opening the system for repair or maintenance.

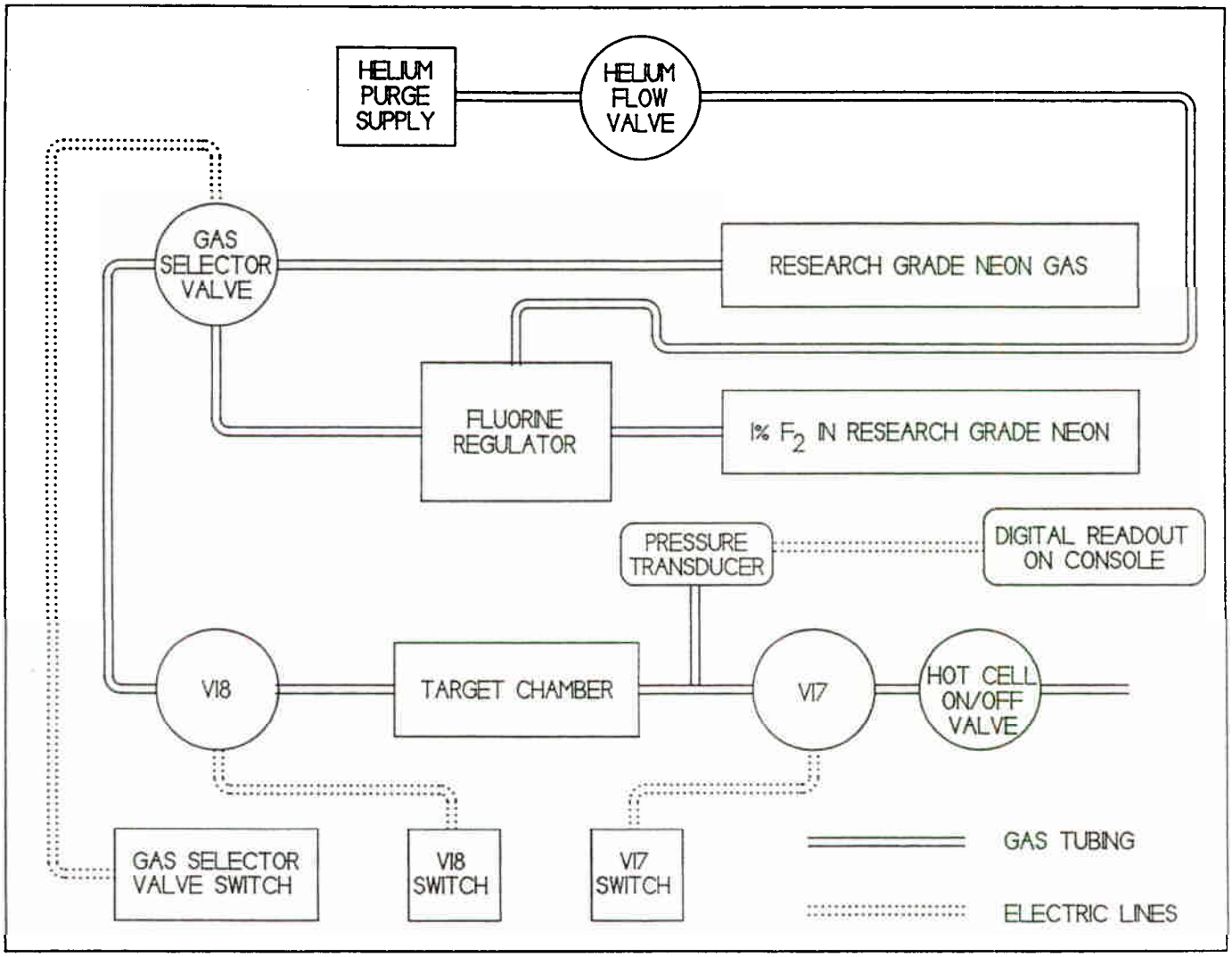

Fig. 2. DIAGRAM SHOWING THE ARRANGEMENT OF SYSTEM COMPONENTS

Initial target treatment consisted of filling the target chamber with 1% F_2 in research grade neon and bombarding the target gas for about 30 minutes at a convenient beam current between 10 and 30 uA. The irradiated target was usually drained from the target chamber through KI solution and the activity retained in the KI was measured. Often a volatile

radioactive component was observed in the first few bombardments after assembly. The absence of a significant volatile radioactive component in the irradiated gas was considered an indication of target operation satisfactory for further experimentation. No passivation of the target chamber with fluorine gas was carried out. The target chamber was flushed by filling and emptying 3 times with 1% F_2 in research grade neon, then 1 time with research grade neon. A selected amount of 1% F_2 in research neon was introduced to the target chamber through V18 (refer to figure 2), followed by pure research grade neon to provide the desired level of F_2 carrier in the target gas. Following bombardment the irradiated gas was immediately drained through an aqueous solution consisting of 5ml of 5% KI, 1ml 1M HCl, 10ml de-ionized water, and a few drops of indicating starch. The target chamber pressure was allowed to drop to about 15 psig during the removal of the irradiated neon, then refilled to about 100 psig with research grade neon and again allowed to empty. Only a single flush was performed. The activity trapped in the KI was measured and the liberated I_2 titrated with $Na_2S_2O_3$ to determine the amount of F_2 recovered. When the target is not to be used for intervals greater than 8 hours it is stored containing about 3 atmospheres of 1% F_2 in research grade neon, or, for routine production, stored containing the normally used bombardment mixture. Target pressure is constantly monitored by a pressure transducer mounted as shown in figure 2.

RESULTS

Little difference in the yields from the two different length target systems was observed. The yields from the long target bombarded at the end of a beam line averaged 23 +/- 3 mCi/uA EOSB (End of Saturation Bombardment) using research grade neon with 0.15 to 0.25 added F_2 and were independent of beam current up to 40.00 uA. The same target mounted directly on a beam exit port provided only slightly lower yields. When about 160 uMoles F_2 are added to the 150 ml target chamber, post bombardment F_2 recovery is 80%, but falls off as the amount of added F_2 is reduced. A similar effect was observed for the short target chamber.

The shorter target chamber provides 22 +/- 5 mCi/uA, EOSB, when mounted on a beam line. The short target chamber has yet to be tested when mounted directly on the cyclotron beam exit port.

In figure 3, the variation of the ratio of target pressure during bombardment to the beam off target pressure at beam currents up to 40 uAmp and a variety of initial (beam off) pressures is presented. For both target configurations the slope of pressure ratio to beam current is very nearly linear, consistent with the yield data indicating the target is thick up to 40 uAmp of beam current, and that only a minimum amount of beam is lost to the target chamber walls. The shorter target chamber has not been run at currents greater than 35 uA with beam off pressure above 120 psig due to the tendency of the foil to burst at pressures above 225 psig. However the data at lower pressure and higher current indicate the target would still be thick.

In the electroformed target chamber both the yield for ^{18}F (mCi/uA, EOSB) and the recovered F_2 are related to the amount of F_2 added to the target gas prior to bombardment. After bombarding the target chamber using up to 260 uMoles F_2 added to the target chamber, a bombardment with no F_2 added to the target gas results in a sharp reduction in the yield of ^{18}F and the recovery of $[^{18}F]$-F_2 to about 15% of the value obtained with carrier.

Fig. 3
BEAM ON/BEAM OFF PRESSURE RATIO
vs. BEAM CURRENT

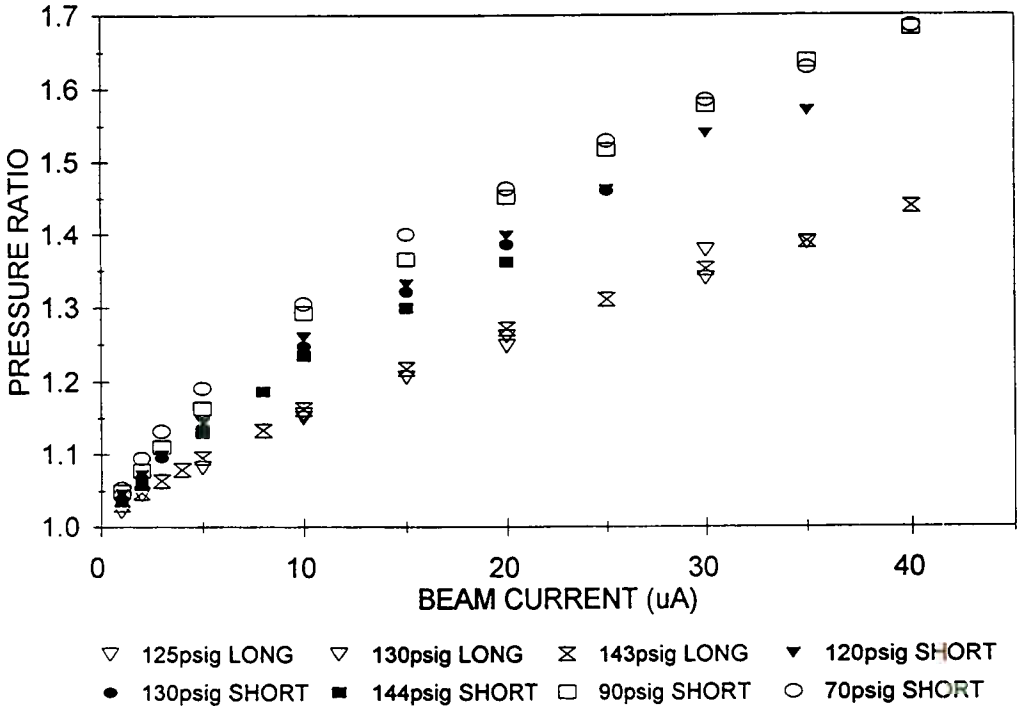

A strong effort was made to relate ^{18}F yield to various experimental parameters, including target pressure, the ratio of target pressure with and without beam, length of bombardment, beam current, amount of F_2 added to the target before bombardment, and the % recovery of the F_2. Trivial and expected correlations of $[^{18}F]$-F_2 yield to beam current, added and recovered F_2 were easily demonstrated. A somewhat more interesting correlation can be seen in figure 4. In figure 4 the yield of $[^{18}F]$-F_2 is shown on the primary ordinate, and the % of input F_2 is shown on the secondary ordinate, as a function of the radiation dose as eV per molecule of added F_2. Data from both target chambers mounted at the end of the beam pipe is presented. The utility of this presentation is that combined in the value of ev/molecule are target pressure, target volume, beam current, particle energy, and duration of bombardment. The data shown come from a wide range of experiments with a variety of conditions. The regression lines for the data shown in figure 4 were compared by standard application of the student's t [8]. At the 95% confidence interval, the regression lines are equivalent, indicating little difference between the two target chambers. The two sets of data were combined and the regression lines for the combined data shown in figure 4 as the heavy solid lines.

Fig. 4
Radionuclide Yield and Carrier Rcvry
vs. Radiation Dose, Long & Short Tgts

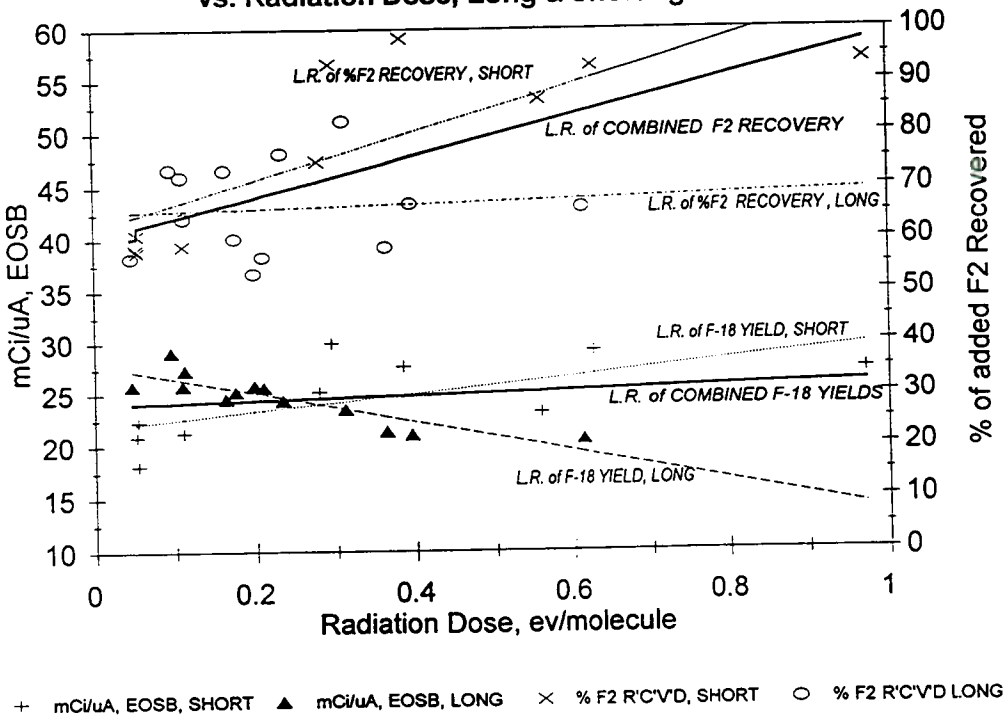

DISCUSSION

Wagner[5] gives a "theoretical value" of 450 mCi at the end of a 110 minute 25 uA bombardment which corresponds with a value of 36 mCi/uA EOSB. The yield from the 150mm target chamber, 23 mCi/uA EOSB and 22 mCi/uA EOSB for the 85 mm target chamber is not significantly different from that reported for the air cooled target chamber, 24 mCi/A EOSB even though there are large differences between the targets. This demonstrates the difficulty in identifying exactly the parameters which are limiting the recovery of $[^{18}F]$-F_2 from deuteron bombarded neon targets, and the still incomplete understanding of all the processes involved. The idea that some of the problems could be attributed to the close proximity of the plasma volume to the target chamber walls is not supported by the data. If the idea were valid, there would be a significant difference between the yields obtained with these targets and the yield from the air-cooled conical target. The longer target was constructed because of concerns [9] that the target may not remain thick to the beam at lower pressures and higher currents. These data indicate the extra length is not needed for targets mounted at the end of a beam pipe. The short target chamber remains untested when mounted directly on the beam exit port.

In figure 4 it can be seen that the combined average ^{18}F yield appears to increase from about 23 mCi/uA EOSB to about 26 mCi/uA EOSB as the radiation dose increases from 0.002 to 1 eV/molecule. Interestingly, the recovery of F_2 increases from about 55% to over 95% over the same interval of radiation dose. These data include variations in the amount carrier F_2 added, the bombardment time, the beam current, and target fill pressures.

CONCLUSION

A simplified cyclotron target system for routine preparation of [^{18}F]-F_2 for clinical 6-[^{18}F]-fluoroDOPA studies, and for other electrophilic fluorinations, via the deuteron bombardment of neon containing less than 0.3% added F_2, has been constructed. The target chamber was designed for use with cyclotrons equipped with a beam line and with cyclotrons where the targets are mounted directly on the beam exit port.

REFERENCES

1) Bida, G.T., Ehrenkaufer, R.L., Wolf, A.P., Fowler, J.S., MacGregor, R.R., Ruth, T.J., The Effect of Target-gas Purity on the Chemical Form of F-18 during ^{18}F-F_2 Production Using the Neon/Fluorine Target, J. Nucl. Med., 21, (8), 758-762, 1980

2) Nickles, R.J., Daube, M.E., Ruth, T.J., An ^{18}O2 Target for the Production of [^{18}F]F_2 Int. J. Radiat. Isot., 35, (2), 117-122, 1984

3) Ruth, T.J., Adam, M.J., Burgerjon.J., Lenz, J., Pate, B.D., A Gas Target for Radionuclide Production with 500 MeV Protons, Int. J. Appl. Rad. & Isot., 36, (12), 931-933, 1985

4) Wieland, B.W., Schlyer, D.J., Wolf, A.P., Charged Particle Penetration in Gas Targets Designed for Accelerator Production of Radionuclides Used in Nuclear Medicine, Int. J. Appl. Radiat. Isot., 35, (5), 387-396, 1984

5) Wagner, R., [Fluorine-18]F_2 Production with 8.5 MeV Deuterons, Proceedings of the IVth International Workshop on Targetry and Target Chemistry, PSI Villigen, Switzerland, Sept. 9-12, 1991

6) Dahl, J.R., Unpublished results.

7) Heselius, S.-J., Lindblom, P., Solin, O., Optical Studies of the Influence of an Intense Ion Beam of High-Pressure Gas Targets., Int. J. Appl. Radiat. Isot. 33:, 6 53-9, 1982.

8) Biostatistical Analysis, 2nd Ed., Zar, J.H., Prentice-Hall Inc. Englewood Cliffs N.J., 1988.

9) Hichwa, R. Personal communication

DETERMINATION OF EXCITATION FUNCTIONS FOR $^{20}Ne(p, p2n)^{18}Ne$ -->^{18}F AND 20Ne(p,2pn)18F AND A REEXAMINATION OF PRODUCTION OF [18F]F_2 WITH PROTONS ON NEON.

G.N. REDDY, H.-F. BEER AND P.A. SCHUBIGER.
DIVISION OF RADIOPHARMACY
PAUL SCHERRER INSTITUTE, CH-5232-VILLIGEN PSI, SWITZERLAND

INTRODUCTION

[^{18}F]F-Labelled radiopharmaceutical continue to play a major role for the development of positron emission tomography (PET) as an *in vivo* modality in biomedical research. The half-life (109.6 min) of [^{18}F]F provides an ideal time for PET investigations. It could be produced in two reactive Forms: a) as nucleophilic fluoride and b) as electrophilic fluorine gas. The most commonly employed two nuclear processes are: $^{20}Ne(d,\alpha)^{18}F$ and $^{18}O(p,n)^{18}F$. The latter process is predominantly used for the production of NCA [^{18}F]fluoride by bombarding [^{18}O]water with protons and has been studied elaborately. The former process is mostly used for the production of carrier-added [^{18}F]F_2 by deuteron bombardment. Generation of [^{18}F]F2 with protons on [^{18}O]O_2 has been implemented, but this method needs optimization.[1,2] Thus, PET centers that do not have dual particle accelerators are limited in methods for the production of [^{18}F]F_2. Nonetheless, the PET centers with medium energy proton (35-40 MeV) cyclotrons, have a better probability for the production of [^{18}F]F_2. It could be generated by $^{20}Ne(p,x)^{18}F$ reaction. This process has not been studied in detail and is being used only at TRIUMPH, UBC PET Center in Vancouver, Canada.[3] At our Institute, two injectors of proton energy 72 MeV are in use for isotope production and hence we examined this nuclear process in detail.

MATERIALS & METHODS

A target made of pure nickel was used for the studies. The cylindrical shaped target was 18.0 cm long with a chamber diameter of 1.8 cm and volume of 64.0 mL. The outer window had a thickness of 0.3 mm and the inner window of 0.5 mm, with 2.2 mm of circulating water for cooling (Figure 1). The production of [^{18}F]F_2 with two different incident proton energies (35 and 39 MeV) was examined. Fixed target pressure of 26 bars that expands upon bombardment to 28 to 31 bars depending on the beam current was used.

One shot and two shoot beam protocols as described by R.J. Nickles et al were implemented.[2] Extracted activity was trapped either in KI solution or NaOAc cartridge and KI solution, unless otherwise mentioned.

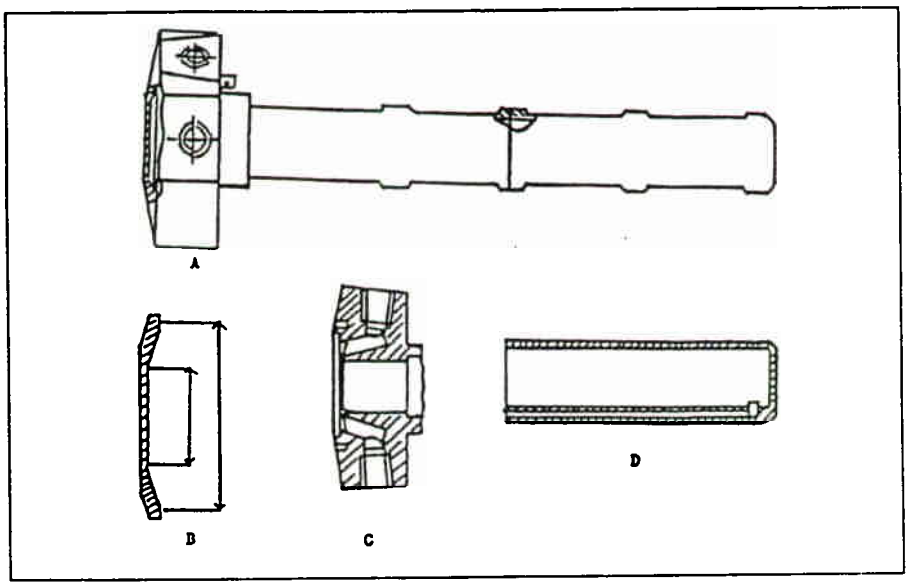

FIGURE 1. SCHEMATIC DLAGRAM OF FLUORNE GAS TARGET:
A) THE OUTLINE OF THE TARGET
B) THE OUTER WINDOW
C) THE INNER WINDOW AND WATER CIRCULATION
D) THE TARGET CHAMBER

RESULTS AND DISCUSSION:

Two modes of production of [^{18}F]F are possible with protons on neon: (a) ^{20}Ne(p, p2n) ^{18}Ne->^{18}F and/or (b) ^{20}Ne(p,2pn)^{18}F. The cross sections for these two reactions are given in Table 1. The excitation functions reach maxima at the proton range of 45-55 MeV for ^{18}Ne and 35-45 MeV for ^{18}F production (Figure 2). However the total cross-section values are similar for the proton range of 25-40 MeV employed for this study. The cross-section values were obtained with ALICE 82, a computer-based evaporation code. Theoretical [^{18}F]F yields from these nuclear reactions were calculated to be approximately 5 mCi /μAh from (p,p2n) and 4 mCi /μAh for (p,2pn) process for the proton range 28-35 MeV and 15 mCi /μAh from (p,p2n) and 12 mCi /μAh for (p,2pn) process for the proton range 28-39 MeV (Table 2 & 3). Straggling of beam was also taken into consideration in these calculations. The instantaneous production rates of ^{18}F for the two reactions are given in Figure 3. Experimentally extracted total values for a two-step protocol are 3-4 mCi /μAh for the proton range 28-35 MeV and 5-6 mCi /μAh . These values represent 30-45% extraction of activity from the target. If the experimental total production values (slightly higher than predicted by code ALICE) were used the extraction values would be lower.[5] However, these amounts allow us to produce routinely carrier-added SFDOPA at our Institute.

TABLE 1. CROSS SECTIONS VALUES FOR ^{18}Ne & ^{18}F.

ENERGY (in MeV)	CROSS SECTIONS (in mbarns)		ENERGY (in MeV)	CROSS SECTIONS (in mbarns)	
	^{18}Ne	^{18}F		^{18}Ne	^{18}F
20	0.0	0.0	26	0.32	0.67
25	0.0	0.0	27	1.26	1.89
30	7.86	4.38	28	2.58	3.47
35	17.05	20.80	29	5.53	3.15
40	27.88	28.36	30	7.86	4.38
45	35.21	26.11	31	12.87	8.16
50	37.21	22.97	32	15.61	10.24
55	35.47	24.11	33	17.38	12.89
60	31.76	22.40	34	20.01	15.16
65	29.19	17.60	35	17.05	20.80
70	26.79	14.63	36	18.78	22.78
75	25.57	13.74	37	21.54	24.65
80	22.71	13.23	38	23.91	26.16
85	21.08	10.40	39	26.47	27.44
90	19.56	9.12	40	27.88	28.39
95	18.84	8.65	41	30.03	24.84
100	16.76	8.80	42	31.52	25.75

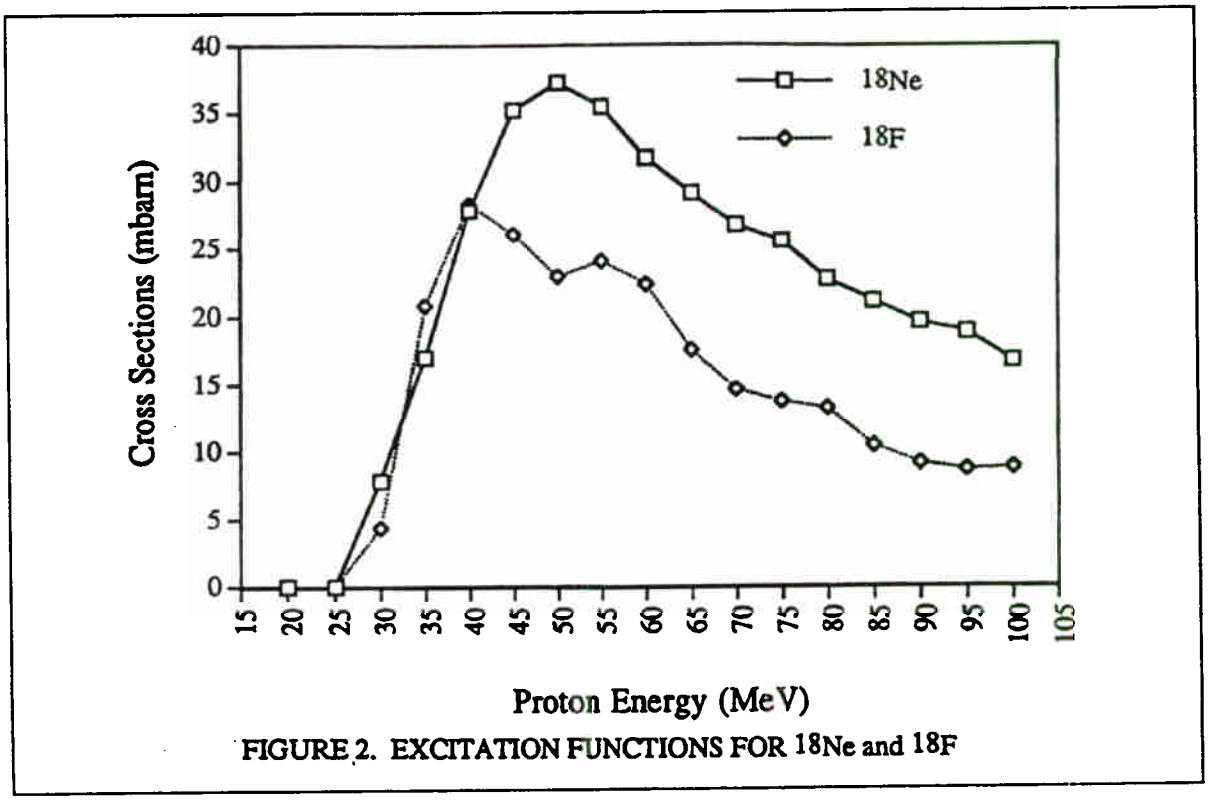

FIGURE 2. EXCITATION FUNCTIONS FOR 18Ne and 18F

TABLE 2: ^{18}F YIELDS AND CROSS SECTIONS FOR $^{20}Ne(p,p2n)^{18}Ne->^{18}F$

Ein	Eout (in MeV)	Emean (mbarn)	Cross sections	Single $^{18}F^{*}$ (mCi/μAh)	Cumulative
39.1	38.1	38.6	21.538	3.623	3.623
38.1	37.2	37.7	18.783	3.096	6.719
37.2	36.2	36.7	17.054	2.752	9.471
36.2	35.3	35.8	20.077	3.182	12.653
35.3	34.3	34.8	17.379	2.699	15.352
34.3	33.3	33.8	15.607	2.362	17.714
33.3	32.4	32.9	12.865	1.902	19.616
32.4	31.5	32.0	7.861	1.137	20.753
31.5	30.5	31.0	5.528	0.781	21.534
30.5	29.6	30.1	2.581	0.361	21.895
29.6	28.6	29.1	1.262	0.170	22.065
28.6	27.7	28.2	0.319	0.042	22.107
27.7	26.7	27.2	0.001	0	22.107

*Based on the assumption that all 18Ne decayed to 18F for long bombardments.

TABLE 3: ^{18}F YIELDS AND CROSS SECTIONS FOR $^{20}Ne(p,2pn)^{18}F$

E_{in}	E_{out} (in MeV)	E_{mean}	Cross sections (mbarn)	Single ^{18}F (mCi/μmAh)	Cumulative
39.1	38.1	38.6	24.648	4.147	4.147
38.1	37.2	37.7	22.782	3.756	7.903
37.2	36.2	36.7	20.797	3.356	11.259
36.2	35.3	35.8	15.156	2.402	13.661
35.3	34.3	34.8	12.886	2.001	15.661
34.3	33.3	33.8	10.236	1.550	17.212
33.3	32.4	32.9	8.159	1.206	18.418
32.4	31.5	32.0	4.38	0.633	19.051
31.5	30.5	31.0	3.149	0.445	19.496
30.5	29.6	30.1	3.47	0.485	19.981
29.6	28.6	29.1	1.889	0.254	20.235
28.6	27.7	28.2	0.668	0.088	20.323
27.7	26.7	27.2	0.002	0	20.323

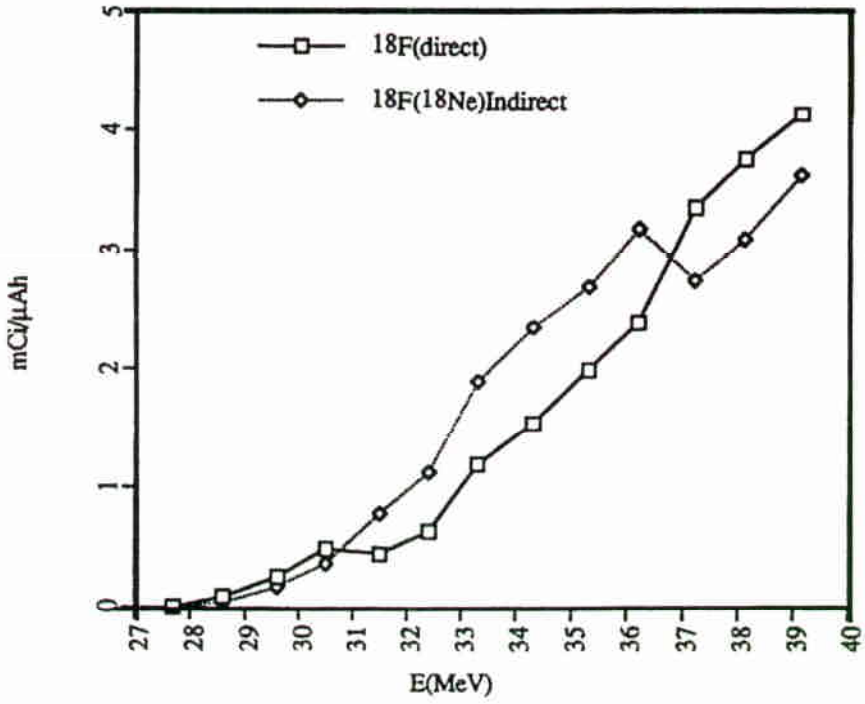

FIGURE 3. 18F PRODUCTION RATE FOR THE TWO REACTIONS

In a two-step production protocol, first the target is filled with pure neon and bombarded for a desired period and is emptied. It is Then filled with desired amount of (carrier) fluorine gas and bombarded again to facilitate exchange between F_2 and [^{18}F]F. It is assumed that during the bombardment [^{18}F]F is generated and deposited onto the inside walls of the target. **However contrary to previous observations, we observe that considerable amount of activity is extracted when pure neon gas alone is bombarded with protons and emptied from the target. When neon gas was emptied directly into a water tank, a violent reaction takes place with the evolution of white dense fumes. The identity of this reactive species is not established. However, we surmise that it is a nascent form of [^{18}F]F that is formed as ^{18}Ne passes through water column. The fumes deposit radioactivity which is that of [^{18}F]F and if the gas is directly trapped from the target, it exhibits initially a high activity which then decays quickly.** If short bombardment periods were employed and the target gas emptied immediately, the above phenomenon is very noticeable. However, if the target gas is emptied after being kept in the target for 5 to 10 min or is emptied through soda lime and charcoal, little or no radioactive gas is observed. We believe that [^{18}F]F activity is not directly generated but indirectly from positron decay of [^{18}Ne]Ne. It is also possible that both processes are taking place at the same time. However due contribution of each process to the total activity is not clear. Studies are underway to characterize the components of the target gas mixture.

CONCLUSION

We have reason to believe that [^{18}F]F is indirectly produced by positron decay of [^{18}Ne]Ne($T_{1/2}$= 1.68 sec) produced by ^{20}Ne(p,p2n) ^{18}F nuclear process.

Acknowledgement:

We thank Dr R. J. Nickles for his help in staring this work and for his helpful discussions. We also thank Drs Hans Reist and Peter Smith Jones for their help in the calculations.

REFERENCES:

1) Bishop A.J., Satyarnunhy N., Bida G., Phelps M.E., BaxTio J.R. J. Nucl. Med. (supply 32, 1010 (1991).
2) Nickles R.J., Daube M.E., Ruth T.J. Appl. Radiat. Isor., 35, 117 (1984).
3) Ruth T.J. Appl. Radial. Isot., 36, 107 (1985). 4) Lagunas-Solar M.C., Haff R.P. Radiochimica Acla, 60, 57 (1993).

Purification of ^{89}Zr using a Hydroxamate Column

W.E. Meijs, J.D.M. Herscheid, H.J. Haisma, P.J. van Leuffen, R. Mooy and H.M. Pinedo.
Radionuclidecentre (RNC), Free University, Amsterdam, The Netherlands

INTRODUCTION

Positron emission tomography (PET) is the best way for non-invasive quantification of the biodistribution of radioisotope-antibody conjugates, required for dosimetric calculations for radioimmunotherapy. The positron emitter ^{89}Zr has good physical characteristics for this application. It has a relatively long half-life (t1/2 = 78.4 h) and decays for 23% by positron emission and for 77% by electron capture to ^{89}Y (stable). The total particle release per desintegration of approximately 100 keV even opens the possibility for therapeutic applications.

EXPERIMENTAL

^{89}Zr was produced in high amounts (130 mCi/h) by a (p,n) reaction on ^{89}Y with 14 MeV protons (97 µA), using the internal radiation facility of a Philips AVF cyclotron. The Y-target was obtained by sputtering ^{89}Y (25 µm, 300 µmol) on a copper target holder. The radionuclidic purity of the ^{89}Zr was very high (>99.99%, table 1).

After production the Zr must be separated from the bulk Y and from Fe, present as a impurity in the Y. For optimizing this separation with a hydroxamate and an anion exchange column (Dowex 2-x8)^{59}Fe and ^{88}Y have been used as tracers. On the hydroxamate column the Fe and Y were completely eluted with 3 M HCl and the Zr was eluted with 1 M oxalic acid (more than 95% in 1 ml, figure 1). The oxalic acid was removed by sublimation at room temperature under vacuum. On the Dowex column the Y was fully eluted with concentrated HCl. Elution with 2 M HCl (40 ml) only gave 80% of the Zr with 60% of the Fe (figure 2). The volume was reduced by evaporation at 60°C.

For labeling antibodies with radiometals, bifunctional chelates are often used. Zr forms very stable complexes with the chelating agent desferal. The chelatability of the Zr with desferal is a good measure for the usefulness of the Zr after purification. After Dowex purification Zr can only be complexated at desferal concentrations of 1 mM or more (figure 3), while after hydroxamate purification the Zr was quantitatively complexated at desferal concentrations in the range necessary for protein labelling (10 µM).

The hydroxamate purification is better than purification on the Dowex column, because of the higher specificity of the hydroxamate column for Zr, giving Zr with less metal pollutants (like Fe) and a higher radionuclidic purity (table 1). Furthermore the hydroxamate column gives higher Zr recovery in less volume and the Zr obtained after hydroxamate purification is more chelatable with desferal.

Table 1. Radionuclidic impurities present in ^{89}Zr-solution at EOB before and after purification (1 hour of irradiation)

element	half-life (days)	production	nCi	nCi impurity after purification	
				Dowex	hydroxamate
^{56}Co	78.8	$^{56}Fe(p,n)$	650	97.5	< 0.5
^{48}V	16.0	$^{48}Ti(p,n)$	3080	52.4	< 3
^{88}Y	106	$^{89}Y(p,pn)$ decay ^{88}Zr	6	< 0.005	< 0.005
^{65}Zn	244	$^{65}Cu(p,n)$	1960	17.64	< 4
^{88}Zr	83.4	$^{89}Y(p,2n)$	2	1.6	1.9
^{89}Zr	3.3	$^{89}Y(p,n)$	$130 * 10^6$	$104 * 10^6$	$123 * 10^6$

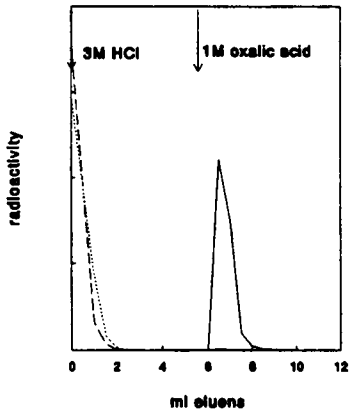

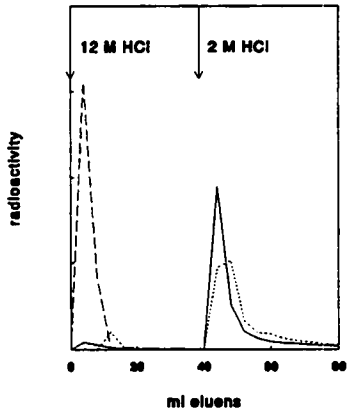

Figures 1 and 2. Purification of Zr(——) from Y(----) and Fe(·····) with a hydroxamate or Dowex column.

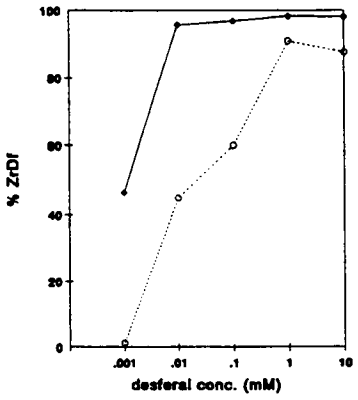

Figure 3. Transchelation curve of Zr with desferal after purification on a Dowex column (·····) and on a hydroxamate column (——).

Nuclear Data Relevant to the Production of ^{67}Ga: A Critical Comparison of Excitation Functions/Thick Target Yield Data for ^{67}Zn(p,n) and ^{68}Zn(p,2n) Nuclear Reactions

F. Szelecsényi, T.E. Boothe, S. Takács*, F. Tárkányi*, E. Tavano, and M. Plitnikas,

Cyclotron Facility, Division of Nuclear Medicine, Mount Sinai Medical Center, Miami Beach, FL. 33140, U.S.A. *Institute of Nuclear Research of the Hungarian Academy of Sciences, Debrecen, Hungary, P.O. Box 51, H-4001

Introduction

The method of choice for routine production of ^{67}Ga on a low energy cyclotron is the ^{67}Zn(p,n)^{67}Ga reaction while above 20 MeV the ^{68}Zn(p,2n)^{67}Ga process results in a higher yield of gallium. To optimize the yields in a production setting it is important to know the cross sections/thick target yield data of these reactions. In spite of the large amount of experimental information on cross section/thick target yield data of the desired reactions published up to 1993, the status in some cases is not satisfactory. In the present work we have compared the available cross sections/thick target yield data and have tried to resolve the most obvious discrepancies which have appeared in the literature. We also present here an evaluated data base for the mentioned data for the ^{67}Zn(p,n)^{67}Ga and ^{68}Zn(p,2n)^{67}Ga nuclear reactions.

During the search for cross sections/thick target yield data the following sources were used: Chemical Abstracts [1], bibliographies of Brookhaven National Laboratory [2] and publications of the International Atomic Energy Agency [3]. The cross sections/thick target yield data used in this compilation were obtained from the original publications except if they were available through the EXFOR data base of the Nuclear Data Section of IAEA. In this case the updated EXFOR values were used for comparison [see reference list]. Unfortunately, in some original works the cross sections and/or thick target yield data were presented only in small figures without tabulation; therefore the use of those values is possible only with the introduction of an additional non-systematic uncertainty both in proton energy scale and in the published values. Due to our inability to accurately read the graphical representations an additional 2-5% error is introduced in these cross section/thick target yield data.

In Table 1 we give a brief summary of the pertinent information used by the authors of the various publications in determination of the cross section and/or yield data, including the investigated energy regions, target types, irradiation arrangements, activity measurements and σ/thick target yield/energy error assessments. The σ and thick target yield data obtained or calculated from all these reports are reproduced in Figs.1-2 for the ^{67}Zn(p,n)^{67}Ga reaction and in Figs.3-4 for the ^{68}Zn(p,2n)^{67}Ga process.

Using the cross sections and thick target yield values of our suggested data bases we also have fitted the excitation functions and yields of the above reactions to get "recommended" values for production planning and nuclear analitical purposes. The fitting procedure was done by using the cubic spline method as follows: a) The individual data sets were fitted separately, then fitted values were calculated for each data set in 0.5 MeV increments. The error of these fitted values in a given energy point was estimated by summing up the error of the nearest experimental value and the deviation of the fitted value in the energy point in question from the

interpolated value calculated from the two nearest experimental data points. b) Weighted average values and their corresponding uncertainties were computed from the fitted ones at each grid points. c) The weighted average was fitted once again and the errors were calculated. These final fitted cross sections/yield values are tabulated in 1 MeV increments in Table 2 and are shown with continuous lines in Figs.1-4. The yields based on integration of the "fitted" excitation curves (using the stopping power of Andersen and Ziegler [12]) are also listed in Table 2.

Excitation function of ^{67}Zn(p,n)^{67}Ga reaction

A survey of the information on cross sections of the above reaction found eight measurements in the literature. All the published results were measured on ^{nat}Zn target except the measurements of Johnson *et al.*[4] and Tárkányi *et al.*[5]. Due to the lack of (p,n), (p,2n) and (p,4n) reaction channel separation, the cross section values measured on ^{nat}Zn targets are useful for comparison only up to 12 MeV. The data of Barrandon *et al.*[6], Blaser *et al.*[7], Bonardi and Birattari [8], Johnson *et al.*[4] and Kopecký [9] were given only in graphical form in the original publications. The systematic investigation of Little and Lagunas-Solar [10] was also done using ^{nat}Zn target, but from the threshold of the ^{68}Zn(p,2n) reaction, separation was made on the basis of systematics of excitation functions of the neighboring nuclei. The cross section values presented by Little and Lagunas-Solar [10] (in 1 MeV increments) were derived from the measured thin target yields. In the most recent publication Nortier *et al.*[11] presented "production cross section" values in tabulated form but without channel separation. We converted the thin target yield data of Bonardi and Birattari [8] to cross section values in the investigated energy region. The cross section data obtained or calculated from all these reports are collected in Fig.1.

On the basis of the available experimental results it can be concluded that the majority of the cross section measurements for ^{67}Zn(p,n)^{67}Ga reaction are in acceptable agreement with each other. However, the peak position of the most *referenced* excitation curve presented by Little and Lagunas-Solar [10] seems to be shifted about 2 MeV towards the high energy direction. The excitation curve of Barrandon *et al.*[6] decreases more rapidly in the tail than the curves of Tárkányi *et al.*[5] (and those of Little and Lagunas-Solar [10]). A possible explanation for the energy shift of Little and Lagunas-Solar [10] was given by Kopecký [9] and Tárkányi *et al.*[5] who supposed a systematic error in foil thicknesses (ie. the foils used by Little and Lagunas-Solar [10] have in average 4% larger thickness than it was reported by them). In an attempt to solve this energy shift problem we have recalculated the proton energy degradation: a) using the reported energy of 35.7 MeV and 0.105 mm thick foils (and the stopping power of Andersen and Ziegler [12]) and b) using a litte lower primary proton energy (35.0 MeV) and the original target thicknesses. Unfortunately, our results can not confirm the supposition of Kopecký [9] and Tárkányi *et al.*[5]. However, the renormalization in the case of lower incident energy moved the foils of the stack to an acceptable energy position in comparison with the values of other groups. It is worth mentioning that supposedly due to the improper channel separation, the new values for the (p,2n) reaction still show some energy shift. Concerning this problem, the corrected (p,n) cross section values of Little and Lagunas-Solar [10] are used for our data base only up to 15 MeV. (Only the original cross section values of Little and Lagunas-Solar [10] are reproduced in Fig.1.) The rapid decrease of the excitation function of Barrandon *et al.*[6] in the tail is probably not correct because the usual shape of a (p,n) reaction is different in this energy region. Due to the problem of the data of Barrandon *et al.*[6] - even if their values

show very good agreement with the results of other groups up to 10 MeV - we rejected them from our data base.

Those cross section values of the different groups which can be used as a cross section data base are marked with closed symbols in Fig.1. The "fitted" cross sections are listed in Table 2 (up to 21 MeV) and are presented with continuous line in Fig.1. On the basis of this fitting the excitation function of the $^{67}Zn(p,n)^{67}Ga$ nuclear reaction shows a maximum of 650 mb at 11 MeV.

Thick target yields of $^{67}Zn(p,n)^{67}Ga$ reaction

In the case of $^{67}Zn(p,n)^{67}Ga$ nuclear reaction eight authors have presented integral thick target yield calculations. Only Dmitriev [13] published his yield data in tabulated form; these were based on the experimental excitation function measurement of Little and Lagunas-Solar [10]. The measured yield values (presented graphically) of Intrator *et al.*[14] originally were defined as the number of radioactive products formed per incident proton upon a thick [stopping] target composed solely of the target isotope. We converted their yield to physical yield values and these converted values are reproduced in Fig.2. Graphical yield results were published by Little and Lagunas-Solar [10] and by Tárkányi *et al.*[5] using their own cross section results. The natural thick target yield data were presented graphically by Barrandon *et al.*[6] ("specific activity curve" was published in the original work which was converted by us), Bonardi [15], Kopecký [9], and Nortier *et al.*[11]. We extrapolated their values to 100% enrichment of ^{67}Zn and presented them up to the threshold energy of the $^{68}Zn(p,2n)^{67}Ga$ reaction in Fig.2. Unfortunately, the excitation function curve "fitting" of Bonardi [15] and Nortier *et al.*[11] were based in both cases on only two measured data point below 12 MeV, therefore their yields have significant errors.

The majority of the presented integral thick target yield calculations show acceptable agreement at lower energies. It was, however, surprising that the data of Intrator *et al.*[14] and Little and Lagunas-Solar [10] (and those of Dmitriev [13]) are systematically higher than the results of Tárkányi *et al.*[5] above 8 and 13 MeV, respectively, which were based on excitation function measurement on highly enriched ^{67}Zn target. It can be supposed that the yield values of Intrator *et al.*[14] contain the contribution of $^{68}Zn(p,2n)$ process (natural Zn targets were irradiated) which contribution can cause these very high yields. Due to this fact their data are excluded from our data set. A small discrepancy can be expected between the yields of Little and Lagunas-Solar [10] and Tárkányi *et al.*[5] on the basis of the "shifted" excitation curve of Little and Lagunas-Solar [10], however, this shifted excitation curve itself cannot explain their high yields. To solve this problem we recalculated the yield of Little and Lagunas-Solar [10] using their "original" cross section values and the stopping power of Andersen and Ziegler [12]. Our recalculation showed an acceptable agreement with the data of Tárkányi *et al.*[5]. On the basis of our recalculation it can be concluded that the thick target yield calculations of Little and Lagunas-Solar [10] are incorrect for the yield of $^{67}Zn(p,n)^{67}Ga$ process. Since the yield data of Dmitriev [13] and Little and Lagunas-Solar [10] are nearly identical, we suppose that Dmitriev [13] did not calculate the mentioned physical yield but only reproduced the yield values of Little and Lagunas-Solar [10] in his work. Thus both the mentioned works are not considered for practical purposes. We have added, however, to our data base those yield values which were based on the corrected cross sections of Little and Lagunas-Solar [10]. These new yield values are not shown in Fig.2. Due to the rapid decrease of the excitation function presented by

Barrandon *et al.*[6] (see previous section) their yields are also excluded from our data base.

In Fig.2 we have marked with closed symbols those yield values of the different groups which can be used as a thick target yield data base. The "fitted" integral thick target yield values are listed up to 21 MeV in Table 2 and are presented with continuous line in Fig.2. The yields calculated using the "fitted" excitation curve of the (p,n) reaction and the stopping power of [12] are also collected in Table 2 (up to 21 MeV).

Excitation function of ^{68}Zn(p,2n)^{67}Ga reaction

For the ^{68}Zn(p,2n)^{67}Ga process eight measurements have been published up to 1993. Although this reaction is the most frequently used for ^{67}Ga production, only two works were found that irradiated highly enriched ^{68}Zn targets to evaluate the cross section data (McGee *et al.*[16] and Tárkányi *et al.*[5]) Both presented their results in numerical form. Barrandon *et al.*[6], Bonardi and Birattari [8], and Kopecký [9] published only "production cross sections" in graphical form. Only Nortier *et al.*[11] tabulated their production cross section results. The values measured on ^{nat}Zn can be used for comparison (simply multiplying the values with 100/18.8) between 13 and 25 MeV. In this range the contribution of ^{67}Zn(p,n)^{67}Ga reaction can be neglected ($<1\%$ at 13 MeV and $\sim$ 5% at 25 MeV) due to the low isotopic abundance of ^{67}Zn in natural zinc matrix and the magnitude of the cross section values of the ^{67}Zn(p,n)^{67}Ga reaction in this energy region (see the section of excitation functions of ^{67}Zn(p,n)^{67}Ga reaction). A single numerical data point was reported in a very early work by Cohen and Newman [17] (780 mb at 21.5 MeV; not reproduced in Fig.3). The systematic investigations of Hermanne *et al.*[18], and Little and Lagunas-Solar [10] were done using channel separation. For subtracting the contribution of ^{67}Zn(p,n)^{67}Ga process, Little and Lagunas-Solar [10] used an earlier mentioned separation method while the procedure of Hermanne *et al.*[18] was not mentioned. We converted the thin target yield data of Bonardi and Birattari [8] to cross section values. The cross sections taken from all these reports are reproduced in Fig.3 (up to 40 MeV).

It can be seen from Fig.3 that the majority of the cross section measurements for the ^{68}Zn(p,2n)^{67}Ga reaction show acceptable agreement with each other in the case of the position of the cross section maxima. However, the σ_{max} values varied in magnitudes: from 420 to 880 mb. Similar to the case of ^{67}Zn(p,n)^{67}Ga reaction the whole curve of Little and Lagunas-Solar [10] seems to be shifted about 2 MeV towards high energy direction. In analyzing the presented experimental results the following can be concluded: Supposedly due to the improper channel separation, Hermanne *et al.*[18] presented enormously high cross section values close to the threshold energy of the (p,2n) reaction. Furthermore, all their cross section values are systematically higher than the results of other groups. Thus we do not use their values for our data base. The problem of the energy shift of Little and Lagunas-Solar [10] was discussed earlier. Their "corrected" values even show a little energy shift of about 1 MeV but are used for our data base. (Only their original data set are reproduced in Fig.3.) The cross section values of McGee *et al.*[16] were calculated using beam fluxes which were based on very old copper monitor reaction of Meadows [19]. The excitation function of the ^{63}Cu(p,n)^{63}Zn and the ^{63}Cu(p,2n)^{62}Zn nuclear reactions measured by Meadows [19] are systematically higher than the presently accepted ones (see Schwerer and Okamoto [20]). We have recalculated the cross section values of McGee *et al.*[16] using the mean of the most concordant monitor reactions mentioned above. Unfortunately, the recalculation resulted in even lower cross section values (10-30%) therefore this data set was also rejected.

Those cross section values of the different groups which can be used as a cross section data base are reproduced with closed symbols in Fig.3. The "fitted" σ values show a peak for the (p,2n) reaction at 20.2 MeV (σ_{max}=631 mb). The numerical data are listed in Table 2 up to 25 MeV and are presented with continuous ($E_p < 25$ MeV) and dotted (25 MeV $< E_p <$ 35 MeV) lines in Fig.3.

Thick target yields of ^{68}Zn(p,2n)^{67}Ga reaction

Four authors have presented integral thick target yield calculation for the above reaction. Dmitriev [13] presented tabulated yield data using the cross sections of Little and Lagunas-Solar [10] and McGee *et al.*[16]. Little and Lagunas-Solar [10] published a yield curve in graphical form based on their own cross section data. Nagame *et al.*[21] calculated thick target yields (in graphical form) expected for a natural zinc target. This calculation was based upon tabulated cross section values of McGee *et al.*[16]. Due to the lack of cross section values for the ^{67}Zn(p,n)^{67}Ga reaction in the original paper of McGee *et al.* [16] this data set also could be used in this section (simply multiplying the values with 100/18.8). However, we believe that the values of McGee *et al.*[16] are not sufficiently detailed to allow an "accurate" thick target yield calculation since they are presented in 5 MeV increments. (See also the problem of their cross section values mentioned in the previous section.) The only thick target yield calculation which is based on σ values measured using enriched ^{68}Zn target was presented graphically by Tárkányi *et al.*[5]. The yield values are collected in Fig.4.

The published yields of Dmitriev [13] and Little and Lagunas-Solar [10] show good agreement with each other over the whole comparable energy region while the data of Nagame *et al.*[21] (above 17 MeV) and Tárkányi *et al.*[5] are lower and higher, respectively, than the values of Dmitriev [13] and Little and Lagunas-Solar [10]. Due to the mentioned energy shift of the excitation function of Little and Lagunas-Solar [10] only the corrected data are useful for our data base. (Only their original yield values are presented in Fig.4.) Since the results of Nagame *et al.*[21] are based on the σ values of McGee *et al.*[16] we rejected these values from our evaluated data base. The values of Dmitriev [13] are also excluded because his calculation is based upon the cross sections of Little and Lagunas-Solar [10] and McGee *et al.*[16].

In Fig.4 we have marked with closed symbols the yield values of Tárkányi *et al.*[5] which can be used without correction for a thick target data base. The "fitted" thick target yield values are listed in Table 2 (up to 25 MeV) and are presented with continuous ($E_p < 25$ MeV) and dotted (25 MeV $< E_p <$ 35 MeV) lines in Fig.4. The yields calculated using the "fitted" excitation curve of the (p,2n) reaction and the stopping power of [12] are also collected in Table 2 (up to 25 MeV) and are shown with dashed line up to 35 MeV in Fig.4.

Conclusion

Cross sections: On the basis of the present compilation, the status of the cross sections of the ^{67}Zn(p,n)^{67}Ga process up to the threshold energy of the ^{68}Zn(p,2n) reactions is good. Additional investigations would be, however, necessary (using highly enriched ^{67}Zn) above 12 MeV to extend this data base because only one author [5] has in this energy region a reliable data set (up to 21 MeV). Due to the mentioned problems in the investigations of Hermanne *et al.*[18], Little and Lagunas-Solar [10] and McGee *et al* [16], the ^{68}Zn(p,2n)^{67}Ga reaction has an acceptable cross section data base only up to 25 MeV. Furthermore, the maxima of the cross

sections needs further evaluation and corrections because even the acceptable works show different maximums (from 580 to 700 mb).

Thick target yields: The selected integral thick target yield calculations can be used as a data base up to 22 and 25 MeV for the (p,n) and (p,2n) reactions, respectively. The small deviations found in the calculated thick target yields originated mainly from the different excitation functions (ie. from the "fitting" of the measured cross sections) and the range-energy tables used for the yield calculations. There is a need to extend these calculations to higher energies (especially in the case of the (p,2n) reaction). Good agreement was found [$<5\%$ in the case of the (p,n) reaction and $<10\%$ for the (p,2n) process] between the yields of the fitted yield curves and the yields based on integration of the fitted excitation curves.

References

[1] *Chemical Abstracts (1947-1992)* American Chemical Society.

[2] *Integral Charged Particle Nuclear Data Bibliography* (Ed. Holden N.E.) BNLNCS-51771 and 5064 and *Accelerator Produced Nuclides for Use in Biology and Medicine* (Eds. Karlstrom K.I. and Christman D.R.) BNL 50448, BNL, Upton, NY, U.S.A.

[3] Gandarias-Cruz D. and Okamoto K. IAEA Report (1988) INDC(NDS)-209/GZ, and Dmitriev P. P. IAEA Report (1986) INDC(CCP)-263/G+CN+SZ.

[4] Johnson C.H. et al. Report ORNL-2910(1960) p.25 [IAEA data file: EXFOR-B0068.011, dated 1978-02-09].

[5] Tárkányi F. et al. *Radiochim.Acta* **50**(1990)19

[6] Barrandon J. N. et al. *Nucl.Instrum.Methods* **127**(1975)269.

[7] Blaser J.-P. et al. *Helv.Phys.Acta* **24**(1951)3 [IAEA data file: EXFOR-B0048.005, dated 1979-01-10].

[8] Bonardi M. and Birattari C. *J.Radioanal.Chem.* **76**(1983)311.

[9] Kopecký P. *Appl.Radiat.Isot.* **41**(1990)606.

[10] Little F. E. and Lagunas-Solar M. C. *Int.J. Appl.Radiat.Isot.* **34**(1983)631 [IAEA data files: EXFOR-A0321.003 and A0321.004, dated 1988-02-18].

[11] Nortier F. M. et al. *Appl.Radiat.Isot.* **42**(1991)353 [IAEA data file: EXFOR-A0498.002, dated 1991-10-25].

[12] Andersen H.H. and Ziegler J.F. *The stopping and ranges of ions in matter.* (1977) Vol.3 (Ed. Ziegler J.F.) p.1. Pergamon, New York, U.S.A.

[13] Dmitriev P. P. IAEA Report (1986) INDC(CCP)-263/G+CN+SZ.

[14] Intrator T. P. et al. *Nucl.Instrum.Method* **188**(1981)347.

[15] Bonardi M. In *Proc.of the IAEA Consultants' Meeting on Data Requirements for Medical Radioisotope Production* IAEA Report (1988) INDC(NDS)-195/GZ p.98

[16] McGee T. et al. *Nucl.Phys.* **A150**(1970)11 [IAEA data file: EXFOR-B0053.003, dated 1985-07-23].

[17] Cohen B. L. and Newman E. *Phys.Rev.* **99**(1955)718 [IAEA data file: EXFOR-B0050.013, dated 1979-01-05].

[18] Hermanne A. et al. In *Proc.of Int.Conf.on Nuclear Data for Science and Technology* (1991) p.616, Springer-Verlag, Berlin [IAEA data file: EXFOR-A0494.005, dated 1991-06-17].

[19] Meadows J. W. *Phys.Rev.* **91**(1953)885.

[20] Schwerer O. and Okamoto K. IAEA Report (1989) INDC(NDS)-218/GZ+.

[21] Nagame Y., Unno M., Nakahara H. and Murakami Y. *Int.J.Appl.Radiat.Isot.* **29**(1978)615.

Table 1. Summary of the experimental circumstances and methods

Author	Investigated reaction	Target	Irradiation	Measurement of activity	σ/yield and energy error	Remarks
Barrandon *et al.* [6]	^{nat}Zn(p,xn): σ meas. from 2.5 to 16 MeV, yield calc. from 6.0 to 16.0 MeV	^{nat}Zn: in CuZn form 10-25 μm,	Van de Graaf and cyclotron: 12 & 20 MeV; Stacked-foil method; Cu monitor reactions for I_{beam}	Ge(Li) detector, 4k MC analyzer, IBM 1800 and 370 computers; No chemical separation	No σ/yield and energy error was reported	"production" σ values and nat. yields were converted by us to enrich. targets
Bonardi & Birattari [8] (see also: Bonardi [15])	^{nat}Zn(p,xn): σ meas. from 6 to 45 MeV, yield calc. from 6.0 to 45.0 MeV	^{nat}Zn: 179 and 4.13 mg/cm^2	Cyclotron: 45 MeV; Stacked-foil method; Current integration	Coaxial Ge(Li) detector 1k MC analyzer; No chemical separation	Differential yields were reported without yield/energy error	Yields & σ values [from diff. yields] were calc. by us to enrich. targets
Blaser *et al.* [7]	^{67}Zn(p,n): σ meas. from 2.3 to 6.4 MeV	^{nat}Zn: 4.7 mg/cm^2	Cyclotron: 6.5 MeV; Stacked-foil method; Current integration	GM counter; No chemical separation	No σ/energy error was reported	Num. σ values were taken from the EXFOR data base
Cohen & Newman [17]	^{68}Zn(p,2n): σ meas. at 21.5 MeV	^{nat}Zn	Cyclotron: 21.5 MeV	Scintillation spectrometer; No chemical separation	Relative σ error: ±15%, in addition to the abs. calibration error: ±15%	
Dmitriev [13]	^{67}Zn(p,n): yield calc. from 6.0 to 40.0 MeV, ^{68}Zn(p,2n): yield calc. from 12 to 94 MeV				No yield/energy error estimation were given	Yield calculations were based on experimental σ data of [10] & [16]
Hermanne *et al.* [18]	^{68}Zn(p,2n): σ meas. from 12 to 40 MeV, yield calc. between 20 and 30 MeV.	^{nat}Zn: 50 μm, e=20 mm [actual surface]	Cyclotron: 9.9 - 42.2 MeV; Stacked-foil method	Coaxial Ge(Li) detector (10% abs. efficiency), MC analyzer; No chemical separation	σ error: ±8.5%, energy error: ±0.6-1.0 MeV	Num. σ values were taken from the EXFOR data base
Intrator *et al.* [14]	^{67}Zn(p,n): yield calc. from 2.3 to 27.0 MeV	^{nat}Zn	Cyclotron: 1.4 - 27 MeV	Ge(Li) detector	Only energy error estimation were given [0.001 %]	Yield as number of ^{67}Ga/incident protons were given (conv. by us to phys. yield)
Johnson *et al.* [4]	^{67}Zn(p,n): σ meas. from 1.85 to 5.34 MeV	Enriched ^{67}Zn (57.2%): 90 keV thick at 3 MeV	Van de Graaf: 5.5 MeV	4π flat-response graphite-sphere det.; No chemical separation	No σ/energy error was reported	Num. σ values were taken from EXFOR data base
Kopecký [9]	^{nat}Zn(p,xn): σ meas. from 4 to 31 MeV, yield calc. from 6.0 to 31.0 MeV	^{nat}Zn: 55.4, 52.6, and 58.3 mg/cm^2 [average thickness] e=2.47 cm	Cyclotron: 31.4±0.2 32.1±0.2, 31.6±0.2 MeV; Stacked-foil method; Current integration, monitor reactions on ^{nat}Cu	Ge(Li) detector [15 cm^3], 64 kbyt analyzator; No chemical separation	σ error: ±5.7-8.5%, yield error: ±12-30% [from 12-30 MeV], energy error in the last foils: ±1.3, ±0.9, ±0.8	The "production" σ values and the natural yields were converted by us to enrich. targets
Little and Lagunas-Solar [10]	^{67}Zn(p,n): σ meas. from 6 to 35.5 MeV, yield calc. from 7 to 36 MeV; ^{68}Zn(p,2n): σ meas. from 14 to 35.5 MeV yield calc. from 16 to 36 MeV	^{nat}Zn thickness: 0.1 mm [area: 1 cm^2]	Cyclotron: 35.7±0.4 MeV; Stacked-foil method	Ge(Li) det, 4k MC analyzer; No chemical separation	Differential yield [σ] error: ±13%; integral yield error: ±13%, no energy error was reported	The diff. yield values were conv. by the Authors to σ. Num. σ values were taken from the EXFOR data base
Nagame *et al.* [21]	^{68}Zn(p,2n): yield calc. from 15 to 32 MeV				No yield/energy error estimation were given	Yield calc. were based on exp. σ data of [16]
Nortier *et al.* [11]	^{nat}Zn(p,xn): σ meas. from 8.4 to 99.6 MeV, yield calc. from 7 to 100 MeV	^{nat}Zn: 100 μm e=19-20 mm	Cyclotron: 100±0.3 66±0.3 and 40±0.2 MeV; Stacked-foil method	HpGe det. [13% rel. efficiency], 8k MC analyzer; No chemical separation	σ error: ±5.7-8.5%; yield error: ±12-30%, energy error: within 1.0 MeV	"production" σ & nat. yields were converted by us to enrich. targets
McGee *et al.* [16]	^{68}Zn(p,2n): σ meas. from 15 to 85 MeV	^{68}Zn (99.3%): in ZnO+CuO+Sc_2O_3 form	Cyclotron:10-85(±2) MeV; Cu monitor reactions for I_{beam}	NaI(Tl) det. 7.5x7.5 cm and 3.75x3.75 cm, 0.4k MCA; Chem. sep.	σ error: ±12-30%	Num. σ values were taken from the EXFOR data
Tárkányi *et al.* [5]	^{67}Zn(p,n): σ meas. from 6.5 to 22 MeV, yield calc. from 7 to 22 MeV; ^{68}Zn(p,2n): σ meas. from to 16 MeV, yield calc. from 2.5 to 22 MeV	^{67}Zn (91.5%), ^{68}Zn (98.9%), 15 mg/cm^2 [average thickness]	Cyclotron: 14, 18 and 22 MeV; Stacked-foil method; Current integration, and monitors	Standard gamma-ray spectroscopy; No chemical separation	σ error: ±12-30% energy error estimated ±0.5 MeV at low energies	

Table 2. Fitted cross sections and thick target yields for the $^{67}Zn(p,n)$ and $^{68}Zn(p,2n)$ nuclear reactions.

Proton energy (MeV)	$^{67}Zn(p,n)^{67}Ga$			$^{68}Zn(p,2n)^{67}Ga$		
	Cross section (mbarn)	Target yield* (mCi/μAh)	Target yield (mCi/μAh)	Cross section (mbarn)	Target yield* (mCi/μAh)	Target yield (mCi/μAh)
2.0	0.37±0.06	0	0	-	-	-
3.0	18.2±3.1	0.002	0	-	-	-
4.0	74.5±10.7	0.013	0.009	-	-	-
5.0	139±14	0.045	0.029	_	-	-
6.0	220±31	0.11	0.07	-	-	-
7.0	328±32	0.21	0.19	-	-	-
8.0	450±39	0.37	0.37	-	-	-
9.0	557±65	0.60	0.59	-	-	-
10.0	627±59	0.89	0.87	-	-	-
11.0	649±0.8	1.23	1.20	-	-	-
12.0	614±1.0	1.58	1.55	-	-	-
13.0	533±125	1.92	1.88	67.5±37.3	0.0098	0
14.0	433±114	2.22	2.17	231±28	0.11	0.06
15.0	340±106	2.47	2.41	361±25	0.31	0.21
16.0	260±94	2.68	2.60	463±32	0.60	0.44
17.0	195±54	2.83	2.75	539±32	0.97	0.77
18.0	147±82	2.96	2.87	589±34	1.41	1.17
19.0	119±35	3.07	2.97	619±34	1.89	1.61
20.0	106±34	3.15	3.05	630±39	2.41	2.07
21.0	101±45	3.24	3.11	625±36	2.94	2.54
22.0	-	-	-	604±45	3.49	3.01
23.0	-	-	-	572±52	4.03	3.48
24.0	-	-	-	534±81	4.55	3.95
25.0	-	-	-	497±100	5.05	4.42

* Target yields were calculated using the "fitted" excitation curves and the stopping power of [12].

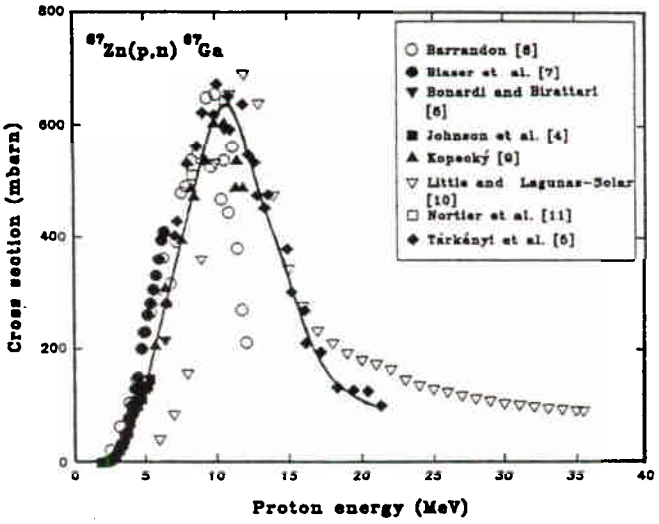

Fig.1. Excitation functions of ^{67}Zn(p,n)^{67}Ga nuclear reaction.

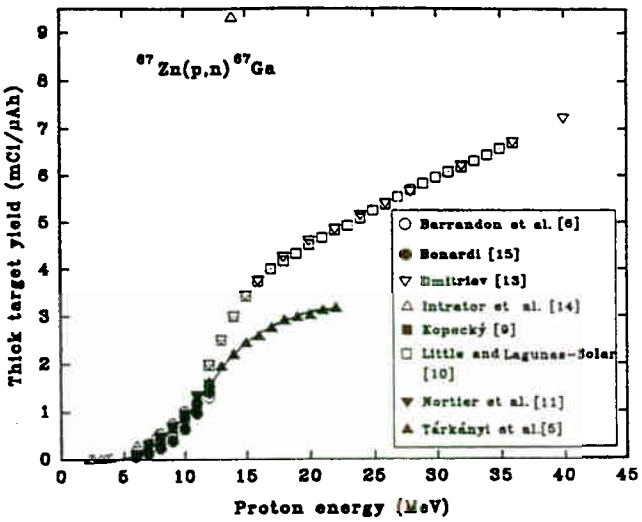

Fig.2. Integral thick target yields of ^{67}Ga for protons on ^{67}Zn.

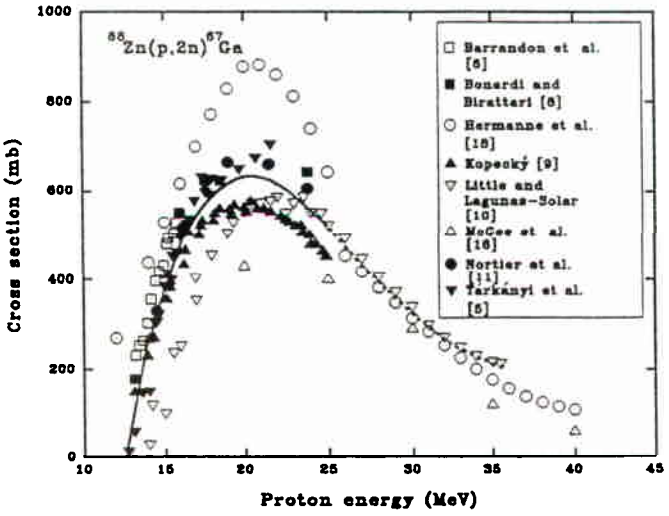

Fig.3. Excitation functions of ^{68}Zn(p,2n)^{67}Ga nuclear reaction.

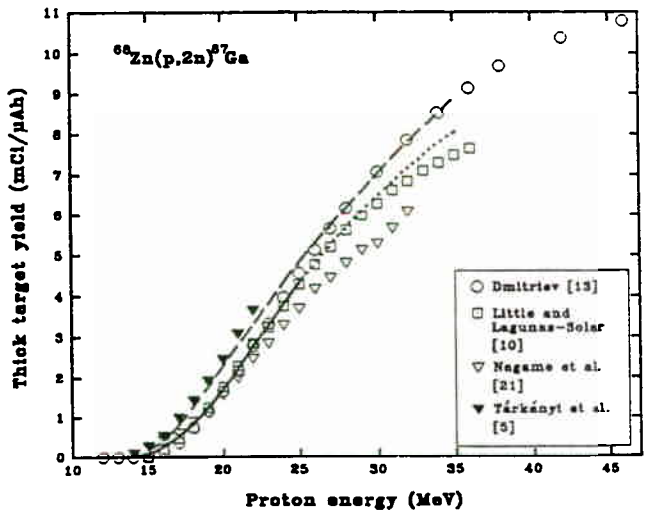

Fig.4. Integral thick target yields of ^{67}Ga for protons on ^{68}Zn.